Available online at www.sciencedirect.com
SCIENCE DIRECT®
Journal of Computational Physics 192 (2003) 643–676
JOURNAL OF COMPUTATIONAL PHYSICS
www.elsevier.com/locate/jcp

Upwind scheme for non-hyperbolic systems

Yao-Hsin Hwang

Chung Shun Institute of Science and Technology, Lung Tan 90008-15-1, Tao Yuan 32526, Taiwan

Received 15 August 2002; received in revised form 15 July 2003; accepted 15 July 2003

Abstract

Upwind scheme has been justified to be an accurate and stable numerical method to solve the hyperbolic system of equations. However, extension of an upwind scheme to solve a non-hyperbolic system may encounter the complex eigensystem in the coefficient matrix. It is difficult to determine the characteristic quantities by the complex eigenvectors and the upwind sense by the complex eigenvalues. Therefore, a suitable transformation is developed in the present work to derive a canonical form for the non-hyperbolic system in the real space. This canonical form will be identical with the characteristic equation if the system becomes hyperbolic. Based on this canonical equation, an upwind scheme can be constructed. This scheme is also extended to include the degenerate system and system with additional inter-drag and diffusion terms. Numerical treatment to avoid the impractically refined time step for a stable computation with a strong inter-drag term is also introduced. Normal-mode analyses are performed to indicate the stability of the proposed scheme and the associated time step constraint for a stable computation. Several representative model equations are solved and the calculated results show that the proposed scheme may be a useful tool to simulate both the hyperbolic and non-hyperbolic system of equations.

Keywords: Upwind scheme; Non-hyperbolic system; Canonical form; Numerical analyses; Inter-drag term

1. Introduction

Upwind scheme has been well established and justified to be an accurate and stable numerical method to solve hyperbolic system of equations. It has been successfully applied to simulate many complicated physical phenomena [1]. To apply the upwind schemes, the equation system is cast into its characteristic form and the upwind sense for the numerical treatment is determined by the eigenvalues arising from the coefficient matrix. Therefore, the applications of a conventional upwind scheme are confined in the hyperbolic equation system. Recently, efforts have been invested by researchers to simulate two-phase flow problems with the upwind schemes [2–4]. However, in some circumstances, the governing two-phase equation system may become non-hyperbolic and the upwind solution procedure will fail due to the

E-mail address: wuwenj@ms29.hinet.net.

0021-9991/$ - see front matter
doi:10.1016/j.jcp.2003.07.014

complex eigensystem inherent in coefficient matrix. It is impossible to find a real characteristic quantity propagating in the space–time domain and the upwind sense required for the numerical scheme cannot be determined by a complex eigenvalue. To surmount this difficulty and fulfill the numerical requirement for upwind schemes, some additional modifications on the virtual mass and interfacial pressure terms in the two-phase model equation are introduced to render the equation system hyperbolic [5,6]. From physical point of view, such a treatment is not necessary for a stable computation. A non-hyperbolic system of two-phase flow problem may also be stabilized with appropriate inter-drag and viscous terms [7]. Therefore, a reasonable solution procedure should be performed directly on the non-hyperbolic system and not on the hypothetically hyperbolic system. Consequently, the prevalent method to solve two-phase model equations is to decouple the system equations into many single equations and solve these equations sequentially [8,9]. Strictly speaking, however, such a segregated treatment for a coupled equation system will not result in a true upwind scheme since the upwind sense should be characterized by the eigenvalues rather than the elements in the coefficient matrix. With a simple numerical analysis, it can be easily shown that this sequential treatment may not guarantee to provide a stable solution even for a linear hyperbolic system. Meanwhile, stable solutions obtained with the sequential methodology may be incurred by excessive numerical diffusion, which will inevitably deteriorate the solution accuracy [10]. This dilemma stimulates the present study to develop a stable and accurate upwind scheme suitable for both the hyperbolic and non-hyperbolic system of equations.

Although the present study is motivated by the unsteady non-hyperbolic two-phase flow problem, it is obvious that methodology proposed in this paper can be employed to solve any type of equation system. For example, one can solve the two-dimensional Laplace equation by rearranging the original equation

$$\frac{\partial \phi}{\partial x^2} + \frac{\partial \phi}{\partial y^2} = 0 \quad \text{as} \quad \frac{\partial \mathbf{U}}{\partial x} + \mathbf{A}\frac{\partial \mathbf{U}}{\partial y} = 0$$

with

$$\mathbf{U} = \left(\frac{\partial \phi}{\partial x}, \frac{\partial \phi}{\partial y}\right)^{\mathrm{T}} \quad \text{and} \quad \mathbf{A} = \begin{pmatrix} 0 & 1 \\ -1 & 0 \end{pmatrix},$$

and by marching the numerical solution in the x-direction. Similar treatment can be found in the error vector propagation (EVP) method proposed by Roache [11] to solve a single elliptic equation. The present method, nevertheless, can solve a single equation as well as the coupled system equations.

Therefore, the main objective of present study is to provide a feasible numerical scheme to solve general hyperbolic or non-hyperbolic systems. Following the same line of reason for the conventional upwind scheme in solving hyperbolic systems, we will derive an associated canonical form for a non-hyperbolic system on which the numerical scheme can be constructed. Besides this section, content of the present paper is organized as follows. Section 2 details the mathematical formulation for the canonical form of a non-degenerate system of equations. Based on this canonical form, the corresponding upwind scheme is derived in Section 3. Numerical analyses are performed to indicate the deficiency of the sequential treatment and show the stability of the proposed scheme. In Section 4, the resulting scheme is extended to include the degenerate equation systems, where the corresponding canonical form is derived with the Jordan decomposition of a coefficient matrix. Effects of inter-drag and viscous terms on the stability of a non-hyperbolic equation system are analyzed in Section 5. A numerical treatment is also introduced to avoid the impractically refined time step for a stable computation with a strong inter-drag term. In Section 6, numerical experiments on solving several representative problems of linear non-degenerate, linear degenerate, non-linear non-degenerate and non-linear degenerate equation systems with the present scheme are performed. Finally, Section 7 is devoted to the conclusions of this study.

2. Canonical form of non-hyperbolic system of equations

For convenience, we first demonstrate the canonical form of a non-degenerate system of equations on which the difference scheme should be constructed. Cases of degenerate systems will be considered in a later section. Therefore, consider the general non-degenerate system of equations

$$\frac{\partial \mathbf{U}}{\partial t} + \mathbf{A}\frac{\partial \mathbf{U}}{\partial x} = \mathbf{0}, \tag{1}$$

where $\mathbf{U}$ is the solution vector in real space, $\mathbf{U} \in \mathbf{R}^{N\times 1}$, and $\mathbf{A}$ is a non-defective real coefficient matrix, $\mathbf{A} \in \mathbf{R}^{N\times N}$, which can then be diagonalized by a non-singular matrix, $\mathbf{L}$ [12],

$$\mathbf{L}\mathbf{A}\mathbf{L}^{-1} = \mathbf{\Lambda} = \mathrm{diag}(\lambda_1, \ldots, \lambda_N). \tag{2a}$$

The ith row in $\mathbf{L}, \mathbf{L}^{(i)}$ is regarded as the ith left eigenvector of $\mathbf{A}$ with respective to the eigenvalue λ_i,

$$\mathbf{L}^{(i)}\mathbf{A} = \lambda_i \mathbf{L}^{(i)}. \tag{2b}$$

It should be noted that the eigenvalues and eigenvectors of $\mathbf{A}$ may be complex, $\lambda_i \in \mathbf{C}$ and $\mathbf{L}^{(i)} \in \mathbf{C}^{1\times N}$. Therefore, the eigensystem can then be designated with its real and imaginary parts:

$$\mathbf{\Lambda} = \mathbf{\Lambda}_R + \mathrm{j}\mathbf{\Lambda}_I, \quad \mathbf{L} = \mathbf{L}_R + \mathrm{j}\mathbf{L}_I, \tag{2c}$$

where subscripts R and I, respectively, denote the real and imaginary parts of a complex quantity and j is the unit imaginary number, $\mathrm{j}^2 = -1$. Since the coefficient matrix, $\mathbf{A}$, is a real matrix, its eigenvalues and associated eigenvectors can be constructed to satisfy the following properties:

(i) If λ_i is real ($\lambda_{i,\mathrm{I}} = 0$), then its associated eigenvector is also real ($\mathbf{L}_\mathrm{I}^{(i)} = \mathbf{0}$).
(ii) If λ_i is complex ($\lambda_{i,\mathrm{I}} \neq 0$), then its complex conjugate λ_j is also an eigenvalue of $\mathbf{A}$. In addition, if their associated eigenvectors are also complex conjugate

$$\lambda_{j,\mathrm{R}} = \lambda_{i,\mathrm{R}}, \quad \lambda_{j,\mathrm{I}} = -\lambda_{i,\mathrm{I}},$$

$$\mathbf{L}_\mathrm{R}^{(i)} = \mathbf{L}_\mathrm{R}^{(\mathrm{j})}, \quad \mathbf{L}_\mathrm{I}^{(i)} = -\mathbf{L}_\mathrm{I}^{(\mathrm{j})},$$

then these two complex conjugate, λ_i and λ_j, can then be designated as a conjugate eigenvalue pair for the real matrix, $\mathbf{A}$.

With the conjugate eigenvalue pair, we can further define a row/column transform matrix, $\mathbf{T}$,

(i) If λ_i is real, $\mathbf{T}^{(i)} = \mathbf{I}^{(i)}$.
(ii) If λ_i is complex and λ_j is its conjugate eigenvalue, $\mathbf{T}^{(i)} = \mathbf{I}^{(j)}$.

In the above relations, $\mathbf{I}$ is the identity matrix and superscript (i) denotes the ith row of a matrix. Therefore, $\mathbf{TM}$ performs a row exchange operation on matrix $\mathbf{M}$,

$(\mathbf{TM})^{(i)} = \mathbf{M}^{(i)}$, if λ_i is a real eigenvalue;
$(\mathbf{TM})^{(i)} = \mathbf{M}^{(j)}$ and $(\mathbf{TM})^{(j)} = \mathbf{M}^{(i)}$, if λ_i and λ_j are the conjugate eigenvalues.

and $\mathbf{MT}$ performs a column exchange operation on matrix $\mathbf{M}$,

$(\mathbf{MT})_{(i)} = \mathbf{M}_{(i)}$, if λ_i is a real eigenvalue;
$(\mathbf{MT})_{(i)} = \mathbf{M}_{(j)}$ and $(\mathbf{MT})_{(j)} = \mathbf{M}_{(i)}$, if λ_i and λ_j are the conjugate eigenvalues.

Subscript (i) denotes the ith column of a matrix.

Based on these properties, we can easily derive the following relations for the eigensystem of matrix, $\mathbf{A}$, by straightforward algebraic manipulations:

$$\text{(i)} \quad \mathbf{TT} = \mathbf{I} \text{ or } \mathbf{T}^{-1} = \mathbf{T}, \tag{3a}$$

$$\text{(ii)} \quad \mathbf{TL}_{\mathrm{R}} = \mathbf{L}_{\mathrm{R}}, \tag{3b}$$

$$\text{(iii)} \quad \mathbf{TL}_{\mathrm{I}} = -\mathbf{L}_{\mathrm{I}}, \tag{3c}$$

$$\text{(iv)} \quad \mathbf{T}\boldsymbol{\Lambda}_{\mathrm{R}}\mathbf{T} = \boldsymbol{\Lambda}_{\mathrm{R}}, \tag{3d}$$

$$\text{(v)} \quad \mathbf{T}\boldsymbol{\Lambda}_{\mathrm{I}}\mathbf{T} = -\boldsymbol{\Lambda}_{\mathrm{I}}, \tag{3e}$$

$$\text{(vi)} \quad \left(\frac{\mathbf{I}+\mathrm{j}\mathbf{T}}{1+\mathrm{j}}\right)\left(\frac{\mathbf{I}-\mathrm{j}\mathbf{T}}{1-\mathrm{j}}\right) = \mathbf{I}, \tag{3f}$$

$$\text{(vii)} \quad \left(\frac{\mathbf{I}+\mathrm{j}\mathbf{T}}{1+\mathrm{j}}\right)(\boldsymbol{\Lambda}_{\mathrm{R}} + \mathrm{j}\boldsymbol{\Lambda}_{\mathrm{I}}) = (\boldsymbol{\Lambda}_{\mathrm{R}} + \boldsymbol{\Lambda}_{\mathrm{I}}\mathbf{T})\left(\frac{\mathbf{I}+\mathrm{j}\mathbf{T}}{1+\mathrm{j}}\right), \tag{3g}$$

$$\text{(viii)} \quad (\mathbf{L}_{\mathrm{R}} + \mathbf{L}_{\mathrm{I}}) = \left(\frac{\mathbf{I}+\mathrm{j}\mathbf{T}}{1+\mathrm{j}}\right)(\mathbf{L}_{\mathrm{R}} + \mathrm{j}\mathbf{L}_{\mathrm{I}}). \tag{3h}$$

Relations (vi) and (viii) also imply that $((\mathbf{I}+\mathrm{j}\mathbf{T})/(1+\mathrm{j}))$ and $(\mathbf{L}_{\mathrm{R}} + \mathbf{L}_{\mathrm{I}})$ are non-singular matrixes. Therefore, substitution of these relations into the original coefficient matrix will lead to the following decomposition:

$$\mathbf{A} = \mathbf{A}_{\mathrm{r}} + \mathbf{A}_{\mathrm{i}} \tag{4a}$$

with

$$\mathbf{A}_{\mathrm{r}} = (\mathbf{L}_{\mathrm{R}} + \mathbf{L}_{\mathrm{I}})^{-1}\boldsymbol{\Lambda}_{\mathrm{R}}(\mathbf{L}_{\mathrm{R}} + \mathbf{L}_{\mathrm{I}}) = \mathbf{L}^{-1}\boldsymbol{\Lambda}_{\mathrm{R}}\mathbf{L}, \tag{4b}$$

$$\mathbf{A}_{\mathrm{i}} = (\mathbf{L}_{\mathrm{R}} + \mathbf{L}_{\mathrm{I}})^{-1}\boldsymbol{\Lambda}_{\mathrm{I}}\mathbf{T}(\mathbf{L}_{\mathrm{R}} + \mathbf{L}_{\mathrm{I}}) = \mathbf{L}^{-1}\boldsymbol{\Lambda}_{\mathrm{I}}\mathbf{T}\mathbf{L} = \mathrm{j}\mathbf{L}^{-1}\boldsymbol{\Lambda}_{\mathrm{I}}\mathbf{L}. \tag{4c}$$

It is interesting to note that although $\mathbf{L}$ is a complex matrix, the resulting matrix, $\mathbf{L}^{-1}\boldsymbol{\Lambda}_{\mathrm{R}}\mathbf{L}$, is a real matrix and equal to $(\mathbf{L}_{\mathrm{R}} + \mathbf{L}_{\mathrm{I}})^{-1}\boldsymbol{\Lambda}_{\mathrm{R}}(\mathbf{L}_{\mathrm{R}} + \mathbf{L}_{\mathrm{I}})$. In this manner, $\mathbf{A}_{\mathrm{r}}$ possesses the same eigenvectors and real part of eigenvalues as the original matrix and $\mathbf{A}_{\mathrm{i}}$ only the imaginary part. Equivalently, the decomposition of a real matrix $\mathbf{A}$ in the real space is

$$\mathbf{A} = (\mathbf{L}_{\mathrm{R}} + \mathbf{L}_{\mathrm{I}})^{-1}(\boldsymbol{\Lambda}_{\mathrm{R}} + \boldsymbol{\Lambda}_{\mathrm{I}}\mathbf{T})(\mathbf{L}_{\mathrm{R}} + \mathbf{L}_{\mathrm{I}}). \tag{5}$$

The original system of equations (1) can then be transformed into the following form:

$$\frac{\partial \mathbf{W}}{\partial t} + \tilde{\boldsymbol{\Lambda}}\frac{\partial \mathbf{W}}{\partial x} = \mathbf{0} \tag{6a}$$

with

$$\tilde{\boldsymbol{\Lambda}} = \boldsymbol{\Lambda}_{\mathrm{R}} + \boldsymbol{\Lambda}_{\mathrm{I}}\mathbf{T} \tag{6b}$$

and

$$\delta\mathbf{W} = \tilde{\mathbf{L}}\delta\mathbf{U} \tag{6c}$$

with

$$\tilde{\mathbf{L}} = \mathbf{L}_{\mathrm{R}} + \mathbf{L}_{\mathrm{I}}, \tag{6d}$$

where $\tilde{\mathbf{\Lambda}}$ and $\tilde{\mathbf{L}}$ can be regarded as the pseudo-eigenvalue and pseudo-eigenvector matrixes for the system of equations, respectively. This is the canonical form for the original system of equations from which several conclusions can be drawn:

(1) This expression can be applied for a general non-degenerate system of equations without regard to its hyperbolicity.
(2) For a hyperbolic system ($\mathbf{\Lambda}_{\mathrm{I}} = \mathbf{L}_{\mathrm{I}} = \mathbf{0}$), it is identical with its characteristic form.
(3) Even for a linear system, it cannot be reduced to many single independent equations as in the hyperbolic case. It requires at least two coupled equations to form a non-hyperbolic system.

3. Numerical scheme

In this section, we will propose a second-order upwind scheme for the non-hyperbolic system of equations. This scheme is based on the canonical form of the equation system (6a)–(6d). However, as mentioned in Section 1, there is an alternative method which decouples the system of equations into many single equations and then solves these equations sequentially. Therefore, before proposing our suitable scheme, we first indicate some deficiency of this method by analyzing its solution for a simple linear hyperbolic system.

3.1. Analysis of sequential treatment

Consider the following linear hyperbolic system of equations:

$$\frac{\partial u}{\partial t} - 5\frac{\partial u}{\partial x} - 21\frac{\partial v}{\partial x} = 0,$$

$$\frac{\partial v}{\partial t} + 2\frac{\partial u}{\partial x} + 8\frac{\partial v}{\partial x} = 0,$$

which indicates the corresponding coefficient matrix

$$\mathbf{A} = \begin{pmatrix} -5 & -21 \\ 2 & 8 \end{pmatrix}.$$

The resulting eigenvalues for this coefficient matrix are $\lambda_1 = 1$ and $\lambda_2 = 2$, which depict a spatially one-way characteristics in the equation system. However, usage of sequential treatment, where the upwind sense is determined by the elements in coefficient matrix, will show a spatially two-way characteristics in the resulting difference equations

$$u_i^{n+1} = u_i^n + \frac{5\Delta t}{\Delta x}(u_{i+1}^n - u_i^n) + \frac{21\Delta t}{\Delta x}(v_{i+1}^n - v_i^n),$$

$$v_i^{n+1} = v_i^n - \frac{2\Delta t}{\Delta x}(u_i^n - u_{i-1}^n) - \frac{8\Delta t}{\Delta x}(v_i^n - v_{i-1}^n),$$

where Δt and Δx are the adopted time step and grid spacing, respectively. By using the standard normal-mode analysis with the following assumed difference solution:

$$u(x,t) = \tilde{u}(t)\exp(\mathrm{j}kx), \quad v(x,t) = \tilde{v}(t)\exp(\mathrm{j}kx),$$

we can find the amplification factor matrix for these difference equations:

$$\tilde{\mathbf{U}}(t+\Delta t) = \mathbf{A}_{\text{num}}\tilde{\mathbf{U}}(t)$$

with $\tilde{\mathbf{U}} = (\tilde{u}, \tilde{v})^{\mathrm{T}}$ and

$$\mathbf{A}_{\text{num}} = \begin{pmatrix} 1 + \frac{5\Delta t}{\Delta x}[\exp(\mathrm{j}k\Delta x) - 1] & \frac{21\Delta t}{\Delta x}[\exp(\mathrm{j}k\Delta x) - 1] \\ -\frac{2\Delta t}{\Delta x}[1 - \exp(-\mathrm{j}k\Delta x)] & 1 - \frac{8\Delta t}{\Delta x}[1 - \exp(-\mathrm{j}k\Delta x)] \end{pmatrix},$$

where k is the imposed wave number with $0 \leqslant k\Delta x \leqslant \pi$. The stability and accuracy of a difference scheme can be analyzed by comparing the numerical amplification factor matrix with the exact one for the differential equation [13]. Therefore, direct numerical computation shows this difference scheme is unstable

$$\max(|\lambda(\mathbf{A}_{\text{num}})|) > 1.$$

That is, from this simple analysis for a linear hyperbolic system of equations, it is shown that the sequential treatment on coupled equations may produce unstable numerical solution. Therefore, it should be very prudent to extend the sequential treatment to solve a general non-hyperbolic system of equations. Such an analysis also illustrates the necessity to develop an accurate and stable method for the non-hyperbolic system.

3.2. Model non-hyperbolic system

Since a non-hyperbolic system is composed of at least two coupled equations, we consider the simplest linear non-hyperbolic system expressed as

$$\frac{\partial u}{\partial t} + \lambda_{\mathrm{R}}\frac{\partial u}{\partial x} + \lambda_{\mathrm{I}}\frac{\partial v}{\partial x} = 0, \tag{7a}$$

$$\frac{\partial v}{\partial t} - \lambda_{\mathrm{I}}\frac{\partial u}{\partial x} + \lambda_{\mathrm{R}}\frac{\partial v}{\partial x} = 0. \tag{7b}$$

Obviously, the eigenvalues for this system are $\lambda_1 = \lambda_{\mathrm{R}} + \mathrm{j}\lambda_{\mathrm{I}}$ and $\lambda_2 = \lambda_{\mathrm{R}} - \mathrm{j}\lambda_{\mathrm{I}}$, which also reveals the following relation:

$$\mathbf{\Lambda} = \mathbf{\Lambda}_{\mathrm{R}} + \mathrm{j}\mathbf{\Lambda}_{\mathrm{I}} = \begin{pmatrix} \lambda_{\mathrm{R}} & 0 \\ 0 & \lambda_{\mathrm{R}} \end{pmatrix} + \mathrm{j}\begin{pmatrix} \lambda_{\mathrm{I}} & 0 \\ 0 & -\lambda_{\mathrm{I}} \end{pmatrix}.$$

Following the same line of reason to develop the upwind scheme for hyperbolic system [14], we will derive the exact solution for these equations and construct its difference counterpart based on this solution. Without loss of generality, we further assume the initial solution

$$u(x,0) = u_0(x) \quad \text{and} \quad v(x,0) = v_0(x), \tag{7c}$$

then the exact solution for these equations can be easily found

$$u(x,t) + \mathrm{j}v(x,t) = u_0(x - \lambda_{\mathrm{R}}t + \mathrm{j}\lambda_{\mathrm{I}}t) + \mathrm{j}v_0(x - \lambda_{\mathrm{R}}t + \mathrm{j}\lambda_{\mathrm{I}}t). \tag{8}$$

Based on this exact solution, an approximate solution can be obtained if the initial distribution around $(x_i = \mathrm{i}\Delta x,\ t = n\Delta t)$ is expressed by the following polynomial:

$$u(x,t) \approx u_i^n + \frac{\delta_x u_i^n}{\Delta x}(x - x_i) + \frac{1}{2}\frac{\delta_x^2 u_i^n}{\Delta x^2}(x - x_i)^2, \tag{9a}$$

$$v(x,t) \approx v_i^n + \frac{\delta_x v_i^n}{\Delta x}(x - x_i) + \frac{1}{2}\frac{\delta_x^2 v_i^n}{\Delta x^2}(x - x_i)^2, \tag{9b}$$

where u_i^n denotes the variable u at $(x_i = i\Delta x, t = n\Delta t)$. The discretized solution at $(x_i, t + \Delta t)$ satisfying the exact solution (8) reads:

$$u_i^{n+1} = u_i^n - \frac{\lambda_R \Delta t}{\Delta x}\delta_x u_i^n - \frac{\lambda_I \Delta t}{\Delta x}\delta_x v_i^n + \frac{1}{2}(\lambda_R^2 - \lambda_I^2)\left(\frac{\Delta t}{\Delta x}\right)^2 \delta_x^2 u_i^n + \lambda_R \lambda_I \left(\frac{\Delta t}{\Delta x}\right)^2 \delta_x^2 v_i^n, \tag{10a}$$

$$v_i^{n+1} = v_i^n - \frac{\lambda_R \Delta t}{\Delta x}\delta_x v_i^n + \frac{\lambda_I \Delta t}{\Delta x}\delta_x u_i^n + \frac{1}{2}(\lambda_R^2 - \lambda_I^2)\left(\frac{\Delta t}{\Delta x}\right)^2 \delta_x^2 v_i^n - \lambda_R \lambda_I \left(\frac{\Delta t}{\Delta x}\right)^2 \delta_x^2 u_i^n, \tag{10b}$$

where δ_x and δ_x^2 represent the first and second spatial differences, respectively,

$$\delta_x u_i = u_{i+1/2} - u_{i-1/2} \quad \text{and} \quad \delta_x^2 u_i = \delta_x u_{i+1/2} - \delta_x u_{i-1/2}. \tag{10c}$$

These two quantities must be appropriately represented by nodal values to give a suitable difference scheme. Eqs. (10a)–(10c) is a second-order accurate numerical approximation for the non-hyperbolic system (7a)–(7c). Furthermore, the approximate solution can be rewritten as

$$\mathbf{W}_i^{n+1} = \mathbf{W}_i^n - \frac{\Delta t}{\Delta x}\tilde{\mathbf{\Lambda}}\delta_x \mathbf{W}_i^n + \frac{1}{2}\left(\frac{\Delta t}{\Delta x}\right)^2 \tilde{\mathbf{\Lambda}}^2 \delta_x^2 \mathbf{W}_i^n \tag{11a}$$

with

$$\mathbf{W} = \begin{pmatrix} u \\ v \end{pmatrix}, \quad \delta_x \mathbf{W} = \begin{pmatrix} \delta_x u \\ \delta_x v \end{pmatrix}, \quad \delta_x^2 \mathbf{W} = \begin{pmatrix} \delta_x^2 u \\ \delta_x^2 v \end{pmatrix} \tag{11b}$$

and the pseudo-eigenvalue matrix, $\tilde{\mathbf{\Lambda}}$, becomes

$$\tilde{\mathbf{\Lambda}} = \mathbf{\Lambda}_R + \mathbf{\Lambda}_I \mathbf{T} = \begin{pmatrix} \lambda_R & \lambda_I \\ -\lambda_I & \lambda_R \end{pmatrix}. \tag{11c}$$

From the discretized representation (11a)–(11c) for the canonical equation (7a)–(7c), the approximation with the same accuracy as for the linear non-hyperbolic system can be equivalently deduced. This is also the basic idea of present work.

3.3. Proposed scheme

Although the above derivation is based on a simple two-equation system, the resulting discretized solution (11a)–(11c) can be equally applied to a general linear system of equations (1) if the eigensystem of coefficient matrix is transformed into its canonical form (6a)–(6d). Following the same methodology employed in solving hyperbolic system, discretized approximation ((10a)–(10c) or (11a)–(11c)) can be rearranged as an two-step upwind scheme:

$$\mathbf{W}_i^{n+1} = \mathbf{W}_i^n - \frac{\Delta t}{\Delta x}\tilde{\mathbf{\Lambda}}(\mathbf{W}_{i+1/2}^{n+1/2} - \mathbf{W}_{i-1/2}^{n+1/2}) \tag{12a}$$

with

$$\mathbf{W}_{i+1/2}^{n+1/2} = \mathbf{W}_{i+1/2}^n - \frac{\Delta t}{2\Delta x}\tilde{\mathbf{\Lambda}}\delta_x \mathbf{W}_{i+1/2}^n \tag{12b}$$

In this way, the inter-grid quantity, $\mathbf{W}_{i+1/2}^{n+1/2}$, can be regarded as the approximate representation for solution vector at $x = (\mathrm{i} + (1/2))\Delta x$ and $t = (n + (1/2))\Delta t$ if the interrelation between discretized spatial and temporal derivatives satisfies the following equation:

$$\delta_t \mathbf{W} + \frac{\Delta t}{\Delta x}\tilde{\mathbf{\Lambda}}\delta_x \mathbf{W} = 0$$

which is also the discretized approximation for the canonical equation (6a)–(6d). In Eq. (12), various discretized representations of $\mathbf{W}_{\mathrm{i}+1/2}^{n}$ and $\delta_x \mathbf{W}_{i+1/2}^{\mathrm{n}}$ will yield different difference schemes. Therefore, to provide an upwind difference scheme, we introduce the left- and right-side expressions for $\mathbf{W}_{i+1/2}^{n+1/2}$ [15]:

$$\mathbf{W}_{i+1/2}^{\mathrm{L}} = \mathbf{W}_i + \left(\frac{\partial \mathbf{W}}{\partial x}\right)_i^{\mathrm{L}} \frac{\Delta x}{2} + \left(\frac{\partial \mathbf{W}}{\partial t}\right)_i^{\mathrm{L}} \frac{\Delta t}{2} = \mathbf{W}_i + \left(\frac{\Delta \mathrm{x}}{2} - \frac{\Delta t}{2}\tilde{\mathbf{\Lambda}}\right)\left(\frac{\partial \mathbf{W}}{\partial x}\right)_i^{\mathrm{L}}, \tag{13a}$$

$$\mathbf{W}_{i+1/2}^{\mathrm{R}} = \mathbf{W}_{i+1} - \left(\frac{\partial \mathbf{W}}{\partial x}\right)_{i+1}^{\mathrm{R}} \frac{\Delta x}{2} + \left(\frac{\partial \mathbf{W}}{\partial t}\right)_{i+1}^{\mathrm{R}} \frac{\Delta t}{2} = \mathbf{W}_{i+1} - \left(\frac{\Delta x}{2} + \frac{\Delta t}{2}\tilde{\mathbf{\Lambda}}\right)\left(\frac{\partial \mathbf{W}}{\partial x}\right)_{i+1}^{\mathrm{R}}. \tag{13b}$$

For the upwind scheme adopted in the present work, this inter-grid quantity in Eq. (12b) can be generalized as

$$\mathbf{W}_{i+1/2}^{n+1/2} = \frac{1}{2}(\mathbf{W}_{i+1/2}^{\mathrm{R}} + \mathbf{W}_{i+1/2}^{\mathrm{L}}) - \frac{1}{2}\tilde{\mathbf{\Lambda}}^{-1}\left|\tilde{\mathbf{\Lambda}}\right|(\mathbf{W}_{i+1/2}^{\mathrm{R}} - \mathbf{W}_{i+1/2}^{\mathrm{L}}) \tag{14}$$

with appropriate selection for $|\tilde{\mathbf{\Lambda}}|$, which will be subsequently described. In the case of hyperbolic system, the absolute function of a diagonal matrix is defined as

$$|\mathbf{\Lambda}| = \mathrm{diag}(|\lambda_1|, |\lambda_2|, \ldots, |\lambda_N|), \tag{15}$$

where all the λ_i are real. For non-hyperbolic system, the modified eigenvalue matrix (6a)–(6d) composed of two parts: $\mathbf{\Lambda}_{\mathrm{R}}$ with all real eigenvalues and $\mathbf{\Lambda}_{\mathrm{I}}\mathbf{T}$ with all imaginary eigenvalues. Therefore, the absolute function of $\mathbf{\Lambda}_{\mathrm{R}}$ is chosen with the identical form (15) to guarantee the same formulation can be equally applied in a hyperbolic system. As for $\mathbf{\Lambda}_{\mathrm{I}}\mathbf{T}$, various forms can be suggested such as in the central difference scheme

$$|\mathbf{\Lambda}_{\mathrm{I}}\mathbf{T}| = \mathbf{0}.$$

However, such a selection will yield two uncoupled difference equation sets if $\mathbf{\Lambda}_{\mathrm{R}} = \mathbf{0}$, which may consequently result in oscillatory solution with deteriorate accuracy. In the present work, we propose the same upwind treatment for $\mathbf{\Lambda}_{\mathrm{I}}\mathbf{T}$ as for $\mathbf{\Lambda}_{\mathrm{R}}$

$$|\mathbf{\Lambda}_{\mathrm{I}}\mathbf{T}| = |\mathbf{\Lambda}_{\mathrm{I}}|\mathbf{T}.$$

Therefore, the adopted absolute function of the modified eigenvalue matrix becomes

$$|\tilde{\mathbf{\Lambda}}| = |\mathbf{\Lambda}_{\mathrm{R}} + \mathbf{\Lambda}_{\mathrm{I}}\mathbf{T}| = |\mathbf{\Lambda}_{\mathrm{R}}| + |\mathbf{\Lambda}_{\mathrm{I}}|\mathbf{T}. \tag{16}$$

Different expressions for the spatial derivatives for the left- and right-side values will lead to various types in the upwind schemes category [14]:

$$\left(\frac{\partial \mathbf{W}}{\partial x}\right)_i^{\mathrm{L}} = 0 \text{ as the first-order upwind scheme (1UD)}, \tag{17a}$$

$$\left(\frac{\partial \mathbf{W}}{\partial x}\right)_i^{\mathrm{L}} = \frac{\mathbf{W}_{i+1}^{n} - \mathbf{W}_i^{n}}{\Delta x} \text{ as the Lax–Wendroff scheme (LW)}, \tag{17b}$$

$$\left(\frac{\partial \mathbf{W}}{\partial x}\right)_i^{\mathrm{L}} = \frac{\mathbf{W}_i^n - \mathbf{W}_{i-1}^n}{\Delta x} \text{ as the Warming–Beam scheme (WB)}, \tag{17c}$$

and

$$\left(\frac{\partial \mathbf{W}}{\partial x}\right)_i^{\mathrm{L}} = \frac{\mathbf{W}_{i+1}^n - \mathbf{W}_{i-1}^n}{2\Delta x} \text{ as the Fromm scheme}, \tag{17d}$$

$(\partial \mathbf{W}/\partial x)_{i+1}^{\mathrm{R}}$ should be treated similarly. All these schemes except 1UD can be easily shown to be second-order accurate with the standard modified equation analysis [13]. For example, adoption of Fromm scheme (17d) will yield the following difference equation (assuming non-negative λ_{R} and λ_{I}):

$$\begin{aligned} u_i^{n+1} = {} & u_i^n - \frac{\lambda_{\mathrm{R}}\Delta t}{\Delta x}(u_i^n - u_{i-1}^n) - \frac{\lambda_{\mathrm{I}}\Delta t}{\Delta x}(v_i^n - v_{i-1}^n) + \frac{\Delta t}{4\Delta x}\left[(\lambda_{\mathrm{R}}^2 - \lambda_{\mathrm{I}}^2)\frac{\Delta t}{\Delta x} - \lambda_{\mathrm{R}}\right](u_{i+1}^n - u_i^n - u_{i-1}^n + u_{i-2}^n) \\ & + \frac{\Delta t}{4\Delta x}\left[2\lambda_{\mathrm{R}}\lambda_{\mathrm{I}}\frac{\Delta t}{\Delta x} - \lambda_{\mathrm{I}}\right](v_{i+1}^n - v_i^n - v_{i-1}^n + v_{i-2}^n), \end{aligned} \tag{18a}$$

$$\begin{aligned} v_i^{n+1} = {} & v_i^n - \frac{\lambda_{\mathrm{R}}\Delta t}{\Delta x}(v_i^n - v_{i-1}^n) + \frac{\lambda_{\mathrm{I}}\Delta t}{\Delta x}(u_i^n - u_{i-1}^n) - \frac{\lambda_{\mathrm{R}}\lambda_{\mathrm{I}}}{4}\left(\frac{\Delta t}{\Delta x}\right)^2(u_{i+1}^n - u_i^n - u_{i-1}^n + u_{i-2}^n) \\ & + \frac{\lambda_{\mathrm{R}}\Delta t}{4\Delta x}\left(\lambda_{\mathrm{R}}\frac{\Delta t}{\Delta x} - 1\right)(v_{i+1}^n - v_i^n - v_{i-1}^n + v_{i-2}^n) - \frac{\lambda_{\mathrm{I}}\Delta t}{4\Delta x}\left(\lambda_{\mathrm{R}}\frac{\Delta t}{\Delta x} + 1\right)(u_{i+2}^n - u_{i+1}^n - u_i^n + u_{i-1}^n) \\ & - \left(\frac{\lambda_{\mathrm{I}}\Delta t}{2\Delta x}\right)^2(v_{i+2}^n - v_{i+1}^n - v_i^n + v_{i-1}^n). \end{aligned} \tag{18b}$$

The equivalent equation system solved by this scheme can be obtained with the Taylor series expansion:

$$\frac{\partial \mathbf{W}}{\partial t} + \tilde{\mathbf{\Lambda}}\frac{\partial \mathbf{W}}{\partial x} = -\frac{1}{2}\left(\frac{\partial^2 \mathbf{W}}{\partial t^2} + \mathbf{M}\frac{\partial^2 \mathbf{W}}{\partial x^2}\right)\Delta t + \mathrm{O}(\Delta t^2), \tag{18c}$$

where

$$\mathbf{M} = \begin{pmatrix} \lambda_{\mathrm{I}}^2 - \lambda_{\mathrm{R}}^2 & -2\lambda_{\mathrm{R}}\lambda_{\mathrm{I}} \\ 2\lambda_{\mathrm{R}}\lambda_{\mathrm{I}} & \lambda_{\mathrm{I}}^2 - \lambda_{\mathrm{R}}^2 \end{pmatrix} = -\tilde{\mathbf{\Lambda}}^2.$$

Therefore, the resulting modified equation becomes

$$\frac{\partial \mathbf{W}}{\partial t} + \tilde{\mathbf{\Lambda}}\frac{\partial \mathbf{W}}{\partial x} = -\frac{1}{2}(\tilde{\mathbf{\Lambda}}^2 + \mathbf{M})\frac{\partial^2 \mathbf{W}}{\partial x^2}\Delta t + \mathrm{O}(\Delta t^2) = \mathrm{O}(\Delta t^2), \tag{18d}$$

which depicts a second-order accurate representation for the original equation system (7a)–(7c). In addition to the above-mentioned linear schemes (17a)–(17d), limiter functions for non-oscillatory solution for hyperbolic system can also be employed as to modify the inter-grid quantities [16]. However, it should be noted that, for an unstable non-hyperbolic system, the limiter function may induce high-frequency components in the resulting numerical solution and rapidly deteriorate the solution accuracy. Therefore, the applications of limiter functions should be confined in solving stable non-hyperbolic equation systems. It is obvious that all the derivations given above are very akin to those for hyperbolic system except the pseudo-eigenvalue matrix, $\tilde{\mathbf{\Lambda}}$.

For the linear system of equations, difference scheme for the transformed variables in the canonical equations can be easily converted into that for the original solution vector. Therefore, if the coefficient matrix is decomposed as in Eqs. (2a)–(2c), the resulting difference scheme for the original equation (1) is

$$\mathbf{U}^{\mathrm{L}}_{i+1/2} = \mathbf{U}_i + \left(\frac{\Delta x}{2} - \frac{\Delta t}{2}\mathbf{A}\right)\left(\frac{\partial \mathbf{U}}{\partial x}\right)^{\mathrm{L}}_i, \tag{19a}$$

$$\mathbf{U}^{\mathrm{R}}_{i+1/2} = \mathbf{U}_{i+1} - \left(\frac{\Delta x}{2} + \frac{\Delta t}{2}\mathbf{A}\right)\left(\frac{\partial \mathbf{U}}{\partial x}\right)^{\mathrm{R}}_{i+1}, \tag{19b}$$

$$\mathbf{U}^{n+1}_i = \mathbf{U}^n_i - \frac{\Delta t}{\Delta x}(\mathbf{F}^N_{i+1/2} - \mathbf{F}^N_{i-1/2}), \tag{19c}$$

$$\mathbf{F}^N_{i+1/2} = \frac{1}{2}\mathbf{A}(\mathbf{U}^{\mathrm{R}}_{i+1/2} + \mathbf{U}^{\mathrm{L}}_{i+1/2}) - \frac{1}{2}(\mathbf{L}_{\mathrm{R}} + \mathbf{L}_{\mathrm{I}})^{-1}(|\mathbf{\Lambda}_{\mathrm{R}}| + |\mathbf{\Lambda}_{\mathrm{I}}|\mathbf{T})(\mathbf{L}_{\mathrm{R}} + \mathbf{L}_{\mathrm{I}})(\mathbf{U}^{\mathrm{R}}_{i+1/2} - \mathbf{U}^{\mathrm{L}}_{i+1/2}), \tag{19d}$$

where $\mathbf{F}^N_{i+1/2}$ represents the numerical flux at $x = (\mathrm{i} + (1/2))\Delta x$. For non-linear conservative equations,

$$\frac{\partial \mathbf{U}}{\partial t} + \frac{\partial \mathbf{F}}{\partial x} = 0, \tag{20a}$$

$$\frac{\partial \mathbf{F}}{\partial \mathbf{U}} = \mathbf{A}, \tag{20b}$$

the above expressions (19a)–(19d) are still applicable, except the numerical flux (19d) being modified as

$$\mathbf{F}^N_{i+1/2} = \frac{1}{2}[\mathbf{F}(\mathbf{U}^{\mathrm{R}}_{i+1/2}) + \mathbf{F}(\mathbf{U}^{\mathrm{L}}_{i+1/2})] - \frac{1}{2}(\mathbf{L}_{\mathrm{R}} + \mathbf{L}_{\mathrm{I}})^{-1}(|\bar{\mathbf{\Lambda}}_{\mathrm{R}}| + |\bar{\mathbf{\Lambda}}_{\mathrm{I}}|\mathbf{T})(\mathbf{L}_{\mathrm{R}} + \mathbf{L}_{\mathrm{I}})(\mathbf{U}^{\mathrm{R}}_{i+1/2} - \mathbf{U}^{\mathrm{L}}_{i+1/2}). \tag{20c}$$

Selection of coefficient matrix between the right and left states should satisfy the general jump condition [17]

$$\bar{\mathbf{A}}(\mathbf{U}_{\mathrm{R}} - \mathbf{U}_{\mathrm{L}}) = \mathbf{F}(\mathbf{U}_{\mathrm{R}}) - \mathbf{F}(\mathbf{U}_{\mathrm{L}}). \tag{20d}$$

3.4. Numerical analysis

The proposed scheme will be reduced to the conventional upwind scheme for a hyperbolic system ($\mathbf{L}_{\mathrm{I}} = \mathbf{\Lambda}_{\mathrm{I}} = \mathbf{0}$). Therefore, it can provide the same stable and accurate results as the conventional upwind scheme if the equation system becomes hyperbolic. In this subsection, we employ the normal-mode analysis to investigate the effects of imaginary part of a complex eigenvalue on the solution stability. For this analysis, consider the solution vector expressed as

$$\mathbf{W}(x,t) = \tilde{\mathbf{W}}(t)\exp(\mathrm{j}kx) \tag{21a}$$

substituted into the model equations (7a)–(7c) to yield the exact amplification matrix

$$\tilde{\mathbf{W}}(t + \Delta t) = \mathbf{A}_{\mathrm{ex}}\tilde{\mathbf{W}}(t) \tag{21b}$$

with

$$\mathbf{A}_{\mathrm{ex}} = \begin{pmatrix} \cosh(C_{\mathrm{I}}\theta) & -\mathrm{j}\sinh(C_{\mathrm{I}}\theta) \\ \mathrm{j}\sinh(C_{\mathrm{I}}\theta) & \cosh(C_{\mathrm{I}}\theta) \end{pmatrix}\exp(-\mathrm{j}C_{\mathrm{R}}\theta), \tag{21c}$$

where C_{R} and C_{I} are the associated Courant number based on the real and imaginary parts of eigenvalues of coefficient matrix, respectively.

$$C_{\mathrm{R}} = \frac{\lambda_{\mathrm{R}}\Delta t}{\Delta x} \quad \text{and} \quad C_{\mathrm{I}} = \frac{\lambda_{\mathrm{I}}\Delta t}{\Delta x}.$$

Without loss of generality, we further assume C_{R} and C_{I} to be non-negative. In the above equation, θ is the dimensionless wave number, $\theta = k\Delta x$.

Characteristics of exact solution can be achieved by the eigenvalues of the exact amplification matrix (21c)

$$\lambda_1(\mathbf{A}_{\mathrm{ex}}) = \exp(C_{\mathrm{I}}\theta)\exp(-\mathrm{j}C_{\mathrm{R}}\theta) \quad \text{and} \quad \lambda_2(\mathbf{A}_{\mathrm{ex}}) = \exp(-C_{\mathrm{I}}\theta)\exp(-\mathrm{j}C_{\mathrm{R}}\theta). \tag{22}$$

Eigenvalues of the exact amplification matrix indicate that solution of a pure non-hyperbolic system will exponentially grow with its growth rate proportional to the wave number, k. From this analysis, one can conclude that real part of complex eigenvalue is responsible for the propagation of information without attenuation. The solution amplification for a pure non-hyperbolic system is completely determined by the imaginary part of complex eigenvalue.

For convenience, characteristics of our proposed scheme will be demonstrated by considering the first-order upwind scheme (17a). As applied to model equations (7a)–(7c), the resulting difference equations become

$$u_i^{n+1} = u_i^n - \frac{\lambda_{\mathrm{R}}\Delta t}{\Delta x}(u_i^n - u_{i-1}^n) - \frac{\lambda_{\mathrm{I}}\Delta t}{\Delta x}(v_i^n - v_{i-1}^n), \tag{23a}$$

$$v_i^{n+1} = v_i^n + \frac{\lambda_{\mathrm{I}}\Delta t}{\Delta x}(u_{i+1}^n - u_i^n) - \frac{\lambda_{\mathrm{R}}\Delta t}{\Delta x}(v_i^n - v_{i-1}^n), \tag{23b}$$

which lead to the amplification matrix,

$$\mathbf{A}_{1\mathrm{UD}} = \begin{pmatrix} 1 - C_{\mathrm{R}}[1 - \exp(-\mathrm{j}\theta)] & -C_{\mathrm{I}}[1 - \exp(-\mathrm{j}\theta)] \\ C_{\mathrm{I}}[\exp(\mathrm{j}\theta) - 1] & 1 - C_{\mathrm{R}}[1 - \exp(-\mathrm{j}\theta)] \end{pmatrix} \tag{24a}$$

and the associated eigenvalues

$$\lambda_1(\mathbf{A}_{1\mathrm{UD}}) = 1 - C_{\mathrm{R}}[1 - \cos(\theta)] + 2C_{\mathrm{I}}\sin\left(\frac{\theta}{2}\right) - \mathrm{j}C_{\mathrm{R}}\sin(\theta), \tag{24b}$$

$$\lambda_2(\mathbf{A}_{1\mathrm{UD}}) = 1 - C_{\mathrm{R}}[1 - \cos(\theta)] - 2C_{\mathrm{I}}\sin\left(\frac{\theta}{2}\right) - \mathrm{j}C_{\mathrm{R}}\sin(\theta). \tag{24c}$$

Because solution for a non-hyperbolic system will grow exponentially, it is suggested that the stability requirement for a numerical scheme should be defined as

$$\max[|\lambda(\mathbf{A}_{\mathrm{num}})|] \leqslant \max\{1, \max[|\lambda(\mathbf{A}_{\mathrm{ex}})|]\}. \tag{25}$$

With the assumed non-negative eigenvalues, the stability criterion for this scheme (23a), (23b) will be

$$|\lambda_{1\mathrm{UD},1}| = |1 - C_{\mathrm{R}}[1 - \cos(\theta)] + 2C_{\mathrm{I}}\sin(\theta/2) - \mathrm{j}C_{\mathrm{R}}\sin(\theta)| \leqslant \exp(C_{\mathrm{I}}\theta) = |\lambda_{\mathrm{ex},1}|. \tag{26}$$

It is very difficult to obtain an explicit expression for the corresponding time step constraint from the stability criterion (26). However, a sufficient condition for the smooth solution ($\theta \to 0$) can be found with approximate series expansion

$$|\lambda_{1\mathrm{UD},1}|^2 \approx 1 + 2C_{\mathrm{I}}\theta + (C_{\mathrm{I}}^2 + C_{\mathrm{R}}^2 - C_{\mathrm{R}})\theta^2 - \frac{1}{12}(C_{\mathrm{I}} + 12C_{\mathrm{R}}C_{\mathrm{I}})\theta^3 + \cdots$$

$$|\lambda_{ex,1}|^2 \approx 1 + 2C_I\theta + 2C_I^2\theta^2 + \frac{4}{3}C_I^3\theta^3 + \cdots$$

Substitution these expressions into the stability criterion (26) will yield the following condition:

$$C_R^2 - C_R - C_I^2 \leqslant 0, \tag{27a}$$

which implies the time step constraint

$$\Delta t \leqslant \frac{\lambda_R \Delta x}{\max(0, \lambda_R^2 - \lambda_I^2)}. \tag{27b}$$

With direct numerical manipulation, we can find that this condition also satisfies the stability criterion (26) in the practical wave number range ($0 \leqslant \theta \leqslant \pi$). Compared with the stability criterion for the hyperbolic systems, it is interesting to note that existence of imaginary part of eigenvalues will dictate a positive effect on the stability of this first-order upwind scheme for the specified wave number. However, it should also be noted that the above stability analysis is based on the imposed wave number and the time-step constraint equations (27a), (27b) may not quarantine a practically stable solution since the information grow rate is dependent on the wave number for an unstable non-hyperbolic system. Any disturbance with high-frequency component will eventually grow and pollute the calculated result. In a later section, this phenomenon will be demonstrated with a numerical example and the time when the high-frequency evolves to overwhelm the useful information can be determined from the amplification matrix.

Similar results can also be derived for the Fromm scheme equations (18a)–(18d), which yields the resulting amplification matrix:

$$\mathbf{A}_{Fromm} = \begin{pmatrix} a_{11} & a_{12} \\ a_{21} & a_{22} \end{pmatrix} \tag{28}$$

with

$$a_{11} = 1 - C_R[1 - \exp(-j\theta)] - \frac{C_R - C_R^2 + C_I^2}{4}[\exp(j\theta) - 1 - \exp(-j\theta) + \exp(-j2\theta)],$$

$$a_{12} = -C_I[1 - \exp(-j\theta)] - \frac{C_R C_I}{4}[\exp(j\theta) - 1 - \exp(-j\theta) + \exp(-j2\theta)],$$

$$a_{21} = C_I[\exp(j\theta) - 1] - \frac{C_R C_I}{4}[\exp(j\theta) - 1 - \exp(-j\theta) + \exp(-j2\theta)] - \frac{C_I + C_R C_I}{4}[\exp(j2\theta) - \exp(j\theta) - 1 + \exp(-j\theta)],$$

$$a_{22} = 1 - C_R[1 - \exp(-j\theta)] - \frac{C_R - C_R^2}{4}[\exp(j\theta) - 1 - \exp(-j\theta) + \exp(-j2\theta)] - \frac{C_I^2}{4}[\exp(j2\theta) - \exp(j\theta) - 1 + \exp(-j\theta)].$$

It is noted that all the above numerical analyses are valid for linear systems. Therefore, analyses of the difference schemes, which are based on the transformed system, can be equally applied to the equivalent original equations.

4. Extension to degenerate system

The above derivations are based on the non-degenerate systems and can be easily extended to solve the degenerate cases. For a general system of equations (1), the coefficient matrix can be decomposed with Jordan decomposition [12]:

$$\mathbf{A} = \mathbf{X}^{-1}\mathbf{J}\mathbf{X} \tag{29a}$$

with

$$\mathbf{J} = \mathrm{diag}(\mathbf{J}_1, \ldots, \mathbf{J}_S), \tag{29b}$$

where $\mathbf{X}$ is a non-singular matrix and the Jordan blocks, $\mathbf{J}_i$, is a $m_i \times m_i$ matrix

$$\mathbf{J}_i = \begin{pmatrix} \lambda_i & 1 & 0 & 0 & 0 & 0 \\ 0 & \lambda_i & 1 & 0 & 0 & 0 \\ 0 & 0 & . & . & 0 & 0 \\ 0 & 0 & 0 & . & . & 0 \\ 0 & 0 & 0 & 0 & \lambda_i & 1 \\ 0 & 0 & 0 & 0 & 0 & \lambda_i \end{pmatrix} \tag{29c}$$

with $m_1 + m_2 + \cdots + m_S = N$ and S is the rank of coefficient matrix $\mathbf{A}$. Although coefficient matrix is a real matrix, the decomposed components, $\mathbf{X}$ and $\mathbf{J}$ may contain complex quantities

$$\mathbf{X} = \mathbf{X}_R + \mathrm{j}\mathbf{X}_I \quad \text{and} \quad \mathbf{J} = \mathbf{J}_R + \mathrm{j}\mathbf{J}_I. \tag{30}$$

Following the same procedure for non-degenerate case, the coefficient matrix can be expressed as

$$\mathbf{A} = (\mathbf{X}_R + \mathbf{X}_I)^{-1}(\mathbf{J}_R + \mathbf{J}_I\mathbf{T})(\mathbf{X}_R + \mathbf{X}_I) \tag{31}$$

and the original system of equations (1) can be transformed into its canonical form

$$\frac{\partial \mathbf{W}}{\partial t} + \tilde{\mathbf{J}}\frac{\partial \mathbf{W}}{\partial x} = \mathbf{0} \tag{32a}$$

with

$$\tilde{\mathbf{J}} = \mathbf{J}_R + \mathbf{J}_I\mathbf{T} \tag{32b}$$

and

$$\delta\mathbf{W} = \tilde{\mathbf{X}}\delta\mathbf{U} \tag{32c}$$

with

$$\tilde{\mathbf{X}} = \mathbf{X}_R + \mathbf{X}_I. \tag{32d}$$

This equation is analogous to the canonical equation for the non-degenerate system (6a)–(6d) except that the eigenvalue matrix is replaced by the Jordan blocks. Therefore, the numerical scheme for a linear non-degenerate system (19a)–(19d) can be easily extended to include the degenerate situation if the numerical flux function (19d) is expressed as

$$\mathbf{F}^N_{i+1/2} = \frac{1}{2}\mathbf{A}(\mathbf{U}^R_{i+1/2} + \mathbf{U}^L_{i+1/2}) - \frac{1}{2}(\mathbf{X}_R + \mathbf{X}_I)^{-1}(|\mathbf{J}_R| + |\mathbf{J}_I|\mathbf{T})(\mathbf{X}_R + \mathbf{X}_I)(\mathbf{U}^R_{i+1/2} - \mathbf{U}^L_{i+1/2}) \tag{33a}$$

with suitable construction for the absolute function of a bi-diagonal matrix, $|\mathbf{J}_{\mathrm{R}}|$

$$|\mathbf{J}_{\mathrm{R}}| = \mathrm{diag}(|J_{1,\mathrm{R}}|, |J_{2,\mathrm{R}}|, \ldots, |J_{S,\mathrm{R}}|) \tag{33b}$$

and

$$|\mathbf{J}_{i,\mathrm{R}}| = \begin{pmatrix} |\lambda_{i,\mathrm{R}}| & 1 & 0 & 0 & 0 & 0 \\ 0 & |\lambda_{i,\mathrm{R}}| & 1 & 0 & 0 & 0 \\ 0 & 0 & . & . & 0 & 0 \\ 0 & 0 & 0 & . & . & 0 \\ 0 & 0 & 0 & 0 & |\lambda_{i,\mathrm{R}}| & 1 \\ 0 & 0 & 0 & 0 & 0 & |\lambda_{i,\mathrm{R}}| \end{pmatrix}. \tag{33c}$$

Similar treatment can be employed for the non-linear conservative equations and the numerical flux function (20c) can be modified as

$$\mathbf{F}^{N}_{i+1/2} = \frac{1}{2}[\mathbf{F}(\mathbf{U}^{\mathrm{R}}_{i+1/2}) + \mathbf{F}(\mathbf{U}^{\mathrm{L}}_{i+1/2})] - \frac{1}{2}(\mathbf{X}_{\mathrm{R}} + \mathbf{X}_{\mathrm{I}})^{-1}(|\mathbf{J}_{\mathrm{R}}| + |\mathbf{J}_{\mathrm{I}}|\mathbf{T})(\mathbf{X}_{\mathrm{R}} + \mathbf{X}_{\mathrm{I}})(\mathbf{U}^{\mathrm{R}}_{i+1/2} - \mathbf{U}^{\mathrm{L}}_{i+1/2}). \tag{33d}$$

To validate the above proposition, we analyze the following simplest degenerate system of equations:

$$\frac{\partial u}{\partial t} + \lambda\frac{\partial u}{\partial x} + \frac{\partial v}{\partial x} = 0, \tag{34a}$$

$$\frac{\partial v}{\partial t} + \lambda\frac{\partial v}{\partial x} = 0 \tag{34b}$$

imposed with the general initial condition (7c). The exact solution for these equations is

$$u(x,t) = u_0(x - \lambda t) - tv_0'(x - \lambda t), \tag{35a}$$

$$v(x,t) = v_0(x - \lambda t), \tag{35b}$$

where

$$v_0^{\cdot}(\eta) = \left.\frac{\mathrm{d}v_0(x)}{\mathrm{d}x}\right|_{x=\eta}. \tag{35c}$$

If the initial distribution is approximated by the polynomial (9a),(9b) and substituted into Eq. (35a)–(35c), the discretized solution at next time step will be

$$u_i^{n+1} = u_i^n - \frac{\lambda\Delta t}{\Delta x}\delta_x u_i^n + \frac{1}{2}\left(\frac{\lambda\Delta t}{\Delta x}\right)^2\delta_x^2 u_i^n - \frac{\Delta t}{\Delta x}\delta_x v_i^n + \lambda\left(\frac{\Delta t}{\Delta x}\right)^2\delta_x^2 v_i^n, \tag{36a}$$

$$v_i^{n+1} = v_i^n - \frac{\lambda\Delta t}{\Delta x}\delta_x v_i^n + \frac{1}{2}\left(\frac{\lambda\Delta t}{\Delta x}\right)^2\delta_x^2 v_i^n, \tag{36b}$$

which can be further rewritten as

$$\mathbf{W}_i^{n+1} = \mathbf{W}_i^n - \frac{\Delta t}{\Delta x}\tilde{\mathbf{J}}\delta_x\mathbf{W}_i^n + \frac{1}{2}\left(\frac{\Delta t}{\Delta x}\right)^2\tilde{\mathbf{J}}^2\delta_x^2\mathbf{W}_i^n, \tag{37}$$

where the solution vector $\mathbf{W}$ is defined as in Eq. (11b). This approximate discretized solution is akin to that for hyperbolic system (11a)–(11c) except that the pseudo-eigenvalue matrix is replaced by the modified Jordan blocks. Therefore, the same difference scheme derived for the non-degenerate coefficient matrix can be equally applied for the degenerate system. Numerical analysis shows the stability criterion for this model equation:

$$C_r = \frac{|\lambda|\Delta t}{\Delta t} \leqslant 1$$

if the first-order scheme is employed.

5. Inter-drag and diffusion terms

As mentioned before, additional inter-drag and diffusion terms may stabilize the non-hyperbolic system. Effects of these terms on the resulting solution can be studied to demonstrate the solution behavior of a stable non-hyperbolic system. For convenience, we consider the following model equations:

$$\frac{\partial u}{\partial t} + \lambda_{\mathrm{R}}\frac{\partial u}{\partial x} + \lambda_{\mathrm{I}}\frac{\partial v}{\partial x} + f_{\mathrm{d}}(u - v) - \mu\frac{\partial^2 u}{\partial x^2} = 0, \tag{38a}$$

$$\frac{\partial v}{\partial t} - \lambda_{\mathrm{I}}\frac{\partial u}{\partial x} + \lambda_{\mathrm{R}}\frac{\partial v}{\partial x} + f_{\mathrm{d}}(v - u) - \mu\frac{\partial^2 v}{\partial x^2} = 0 \tag{38b}$$

or expressed in vector form:

$$\frac{\partial \mathbf{W}}{\partial t} + \mathbf{A}\frac{\partial \mathbf{W}}{\partial x} + \mathbf{C}\mathbf{W} - \mu\frac{\partial^2 \mathbf{W}}{\partial x^2} = 0 \tag{39a}$$

with

$$\mathbf{W} = \begin{pmatrix} u \\ v \end{pmatrix}, \quad \mathbf{A} = \begin{pmatrix} \lambda_{\mathrm{R}} & \lambda_{\mathrm{I}} \\ -\lambda_{\mathrm{I}} & \lambda_{\mathrm{R}} \end{pmatrix} \quad \text{and} \quad \mathbf{C} = f_{\mathrm{d}}\begin{pmatrix} 1 & -1 \\ -1 & 1 \end{pmatrix}, \tag{39b}$$

where f_{d} and μ are the non-negative inter-drag and diffusion coefficients, respectively. Effect of inter-drag term is to decrease the difference between solution vectors; whereas, the diffusion term will decrease the spatial gradient of solution vectors. Using the same normal-mode analysis and substituting the exact solution

$$\mathbf{W}(x,t) = \tilde{\mathbf{W}}(t)\exp[\mathrm{j}k(x - \lambda_{\mathrm{R}}t)] \tag{40a}$$

into the differential equation (38), the associated equation for the solution amplitude $\tilde{\mathbf{W}}(t)$ can be found

$$\frac{\mathrm{d}\tilde{\mathbf{W}}}{\mathrm{d}t} + \tilde{\mathbf{A}}\tilde{\mathbf{W}} = 0 \tag{40b}$$

with

$$\tilde{\mathbf{A}} = \begin{pmatrix} f_{\mathrm{d}} + \mu k^2 & \mathrm{j}k\lambda_{\mathrm{I}} - f_{\mathrm{d}} \\ -\mathrm{j}k\lambda_{\mathrm{I}} - f_{\mathrm{d}} & f_{\mathrm{d}} + \mu k^2 \end{pmatrix}. \tag{40c}$$

Eigenvalues of $\tilde{\mathbf{A}}$ are

$$\tilde{\lambda}_1(\tilde{\mathbf{A}}) = f_d + \mu k^2 + \sqrt{f_d^2 + k^2\lambda_I^2}, \tag{41a}$$

$$\tilde{\lambda}_2(\tilde{\mathbf{A}}) = f_d + \mu k^2 - \sqrt{f_d^2 + k^2\lambda_I^2}. \tag{41b}$$

It is worth noting that the amplitude evolution matrix, $\tilde{\mathbf{A}}$, does not influenced by the real part of complex eigenvalues, λ_R. That is, λ_R determines the information propagation speed and does not affect its evolution amplitude. This phenomenon can also be observed in the pure non-hyperbolic system (22). The stability criterion for the system is that all eigenvalues of $\tilde{\mathbf{A}}$ must be non-negative. This criterion leads to the following relation:

$$\mu^2 k^4 + (2\mu f_d - \lambda_I^2)k^2 \geqslant 0. \tag{42}$$

Based on this condition, several interesting conclusions can be drawn for the non-hyperbolic system with $\lambda_I \neq 0$:

(i) If the system is without diffusion term ($\mu = 0$), it will be still unstable. That is, existence of diffusion term is a necessary condition to stabilize the non-hyperbolic system.

(ii) If the system is without inter-drag term ($f_d = 0$), solution with high wave number, $k \geqslant \lambda_I/\mu$, will be stabilized; nevertheless, low frequency solution is still unstable.

(iii) For any combination of inter-drag and diffusion terms, the critical wave number can be found:

$$k_{CR} = \sqrt{(\lambda_I^2 - 2\mu f_d)/\mu^2}. \tag{43a}$$

Solution can be stabilized if the imposed wave number larger than the critical one, $k > k_{CR}$.

(iv) The condition for a stable solution can be derived by requiring stability for all wave-number k in Eq. (42)

$$\mu f_d \geqslant \frac{1}{2}\lambda_I^2, \tag{43b}$$

which also implies the required viscosity to stabilized all wave-number without inter-drag term will become infinity. In other words, a system without diffusion term is always unstable and a stable system must possess both the inter-drag and diffusion terms. It is easier to stabilize a solution with high wave number than with low wave number. These conclusions can be further employed to interpret the numerical results in this study.

The numerical treatments for these terms are not trivial, since the effects of inter-drag term may result in an impractically refined time step for a stable solution. This is the so-called stiff problem in the equation system with significant source terms. To avoid such a disadvantage, we employ the exponential time differencing [18] and rearrange the original equation system

$$\frac{\partial \mathbf{U}}{\partial t} + \mathbf{A}\frac{\partial \mathbf{U}}{\partial x} + \mathbf{C}\mathbf{U} - \mu\frac{\partial^2 \mathbf{U}}{\partial x^2} = \mathbf{0} \tag{44a}$$

as

$$\frac{\partial \mathbf{U}^*}{\partial t} + \mathbf{A}^*\frac{\partial \mathbf{U}^*}{\partial x} - \mu\frac{\partial^2 \mathbf{U}^*}{\partial x^2} = \mathbf{0} \tag{44b}$$

by setting

$$\mathbf{U}^* = \exp(\mathbf{C}t)\mathbf{U} \quad \text{and} \quad \mathbf{A}^* = \exp(\mathbf{C}t)\mathbf{A}\exp(-\mathbf{C}t). \tag{44c}$$

In Eqs. (44a)–(44c), the stiff problem due to inter-drag term has been eliminated. The numerical scheme (19a)–(19d) should be modified as

$$\mathbf{U}^{\mathrm{L}}_{i+1/2} = \exp\left(-\mathbf{C}\frac{\Delta t}{2}\right)\left[\mathbf{U}^n_i + \left(\frac{\Delta x}{2} - \frac{\Delta t}{2}\mathbf{A}\right)\left(\frac{\partial \mathbf{U}}{\partial x}\right)^{\mathrm{L}}_i + \mu\frac{\Delta t}{2}\left(\frac{\partial^2 \mathbf{U}}{\partial x^2}\right)^n_i\right], \tag{45a}$$

$$\mathbf{U}^{\mathrm{R}}_{i-1/2} = \exp\left(-\mathbf{C}\frac{\Delta t}{2}\right)\left[\mathbf{U}^n_i - \left(\frac{\Delta x}{2} + \frac{\Delta t}{2}\mathbf{A}\right)\left(\frac{\partial \mathbf{U}}{\partial x}\right)^{\mathrm{R}}_i + \mu\frac{\Delta t}{2}\left(\frac{\partial^2 \mathbf{U}}{\partial x^2}\right)^n_i\right], \tag{45b}$$

where $(\partial \mathbf{U}/\partial x)^{\mathrm{L}}_i$ and $(\partial \mathbf{U}/\partial x)^{\mathrm{R}}_i$ are given as in Eqs. (17a)–(17d) and $(\partial^2 \mathbf{U}/\partial x^2)^n_i$ can be represented by the central-difference form

$$\left(\frac{\partial^2 \mathbf{U}}{\partial x^2}\right)^n_i = \frac{\mathbf{U}^n_{i+1} - 2\mathbf{U}^n_i + \mathbf{U}^n_{i-1}}{\Delta x^2}. \tag{45c}$$

We further define

$$\tilde{\mathbf{U}}_i = \frac{1}{2}(\mathbf{U}^{\mathrm{L}}_{i+1/2} + \mathbf{U}^{\mathrm{R}}_{i-1/2}) \tag{45d}$$

and the resulting difference expression is

$$\mathbf{U}^{n+1}_i = \exp(-\mathbf{C}\Delta t)\mathbf{U}^n_i - \frac{\Delta t}{\Delta x}\exp\left(-\mathbf{C}\frac{\Delta t}{2}\right)\left[\mathbf{F}^C_{i+1/2} - \mathbf{F}^C_{i-1/2} - \mathbf{F}^D_{i+1/2} + \mathbf{F}^D_{i-1/2}\right], \tag{45e}$$

where the convective flux, $\mathbf{F}^C_{i+1/2}$, is given as in Eq. (19d) and the diffusive flux, $\mathbf{F}^D_{i+1/2}$, is expressed as

$$\mathbf{F}^D_{i+1/2} = \mu\frac{\tilde{\mathbf{U}}_{i+1} - \tilde{\mathbf{U}}_i}{\Delta x}. \tag{45f}$$

For the non-linear system

$$\frac{\partial \mathbf{U}}{\partial t} + \frac{\partial \mathbf{F}}{\partial x} + \mathbf{C}\mathbf{U} - \mu\frac{\partial^2 \mathbf{U}}{\partial x^2} = \mathbf{0} \tag{46a}$$

and

$$\frac{\partial \mathbf{F}}{\partial \mathbf{U}} = \mathbf{A}. \tag{46b}$$

Eqs. (45a) and (45b) should be modified as

$$\mathbf{U}^{\mathrm{L}}_{i+1/2} = \exp\left(-\mathbf{C}^n_i\frac{\Delta t}{2}\right)\left[\mathbf{U}^n_i + \left(\frac{\Delta x}{2} - \frac{\Delta t}{2}\mathbf{A}^n_i\right)\left(\frac{\partial \mathbf{U}}{\partial x}\right)^{\mathrm{L}}_i + \mu\frac{\Delta t}{2}\left(\frac{\partial^2 \mathbf{U}}{\partial x^2}\right)^n_i\right], \tag{47a}$$

$$\mathbf{U}^{\mathrm{R}}_{i-1/2} = \exp\left(-\mathbf{C}^n_i\frac{\Delta t}{2}\right)\left[\mathbf{U}^n_i - \left(\frac{\Delta x}{2} + \frac{\Delta t}{2}\mathbf{A}^n_i\right)\left(\frac{\partial \mathbf{U}}{\partial x}\right)^{\mathrm{R}}_i + \mu\frac{\Delta t}{2}\left(\frac{\partial^2 \mathbf{U}}{\partial x^2}\right)^n_i\right] \tag{47b}$$

with

$$\mathbf{C}^n_i = \mathbf{C}(\mathbf{U}^n_i) \quad \text{and} \quad \mathbf{A}^n_i = \mathbf{A}(\mathbf{U}^n_i) \tag{47c}$$

and Eq. (45e) modified as

$$\mathbf{U}_i^{n+1} = \exp\left(-\tilde{\mathbf{C}}_i\Delta t\right)\mathbf{U}_i^n - \frac{\Delta t}{\Delta x}\exp\left(-\tilde{\mathbf{C}}_i\frac{\Delta t}{2}\right)\left[\mathbf{F}^C_{i+1/2} - \mathbf{F}^C_{i-1/2} - \mathbf{F}^D_{i+1/2} + \mathbf{F}^D_{i-1/2}\right] \tag{47d}$$

with

$$\tilde{\mathbf{C}}_i = \mathbf{C}(\tilde{\mathbf{U}}_i). \tag{47e}$$

Although there may exist other possible expressions for the intermediate quantities in (45d), (47c) and (47e), they are chosen in these simple forms to yield a second-order accurate difference expression for original equation (44a). With some necessary symbolic manipulations, it can be shown that this expression will lead to a second-order accurate scheme. For example, the Fromm scheme (17d) will yield the following equivalent equation:

$$\frac{\partial \mathbf{U}}{\partial t} + \mathbf{A}\frac{\partial \mathbf{U}}{\partial x} + \mathbf{C}\mathbf{U} - \mu\frac{\partial^2 \mathbf{U}}{\partial x^2} = -\frac{1}{2}\left[\frac{\partial^2 \mathbf{U}}{\partial t^2} - \mathbf{C}^2\mathbf{U} - (\mathbf{A}\mathbf{C} + \mathbf{C}\mathbf{A})\frac{\partial \mathbf{U}}{\partial x} - (\mathbf{A}^2 - 2\mu\mathbf{C})\frac{\partial^2 \mathbf{U}}{\partial x^2} + 2\mu\mathbf{A}\frac{\partial^3 \mathbf{U}}{\partial x^3} - \mu^2\frac{\partial^4 \mathbf{U}}{\partial x^4}\right]\Delta t + \mathrm{O}(\Delta t^2). \tag{48}$$

Using the standard procedure to derive modified equation [13], the resulting modified equation can be shown to be a second-order accurate representation for the original equation (44a)

$$\frac{\partial \mathbf{U}}{\partial t} + \mathbf{A}\frac{\partial \mathbf{U}}{\partial x} + \mathbf{C}\mathbf{U} - \mu\frac{\partial^2 \mathbf{U}}{\partial x^2} = \mathrm{O}(\Delta t^2). \tag{49}$$

Although this scheme is formerly second-order accurate, it requires much computational load due to the existence of diffusion term. Therefore, to alleviate the computational burden, this scheme may be relaxed such that the diffusive term in equations (45a), (45b), (47a) and (47b) are neglected and the diffusive flux shown in Eq. (45f) is modified as

$$\mathbf{F}^D_{i+1/2} = \mu\frac{\mathbf{U}^n_{i+1} - \mathbf{U}^n_i}{\Delta x}. \tag{50}$$

Although the formal accuracy of the relaxed scheme is reduced to first-order, it is shown that the differences in computational results between the complete and relaxed schemes are insignificant. Numerical evidence on the solution accuracy will be given in the following section.

6. Numerical tests

To validate the usefulness of our proposed scheme, we performed a series of numerical computations on several test examples including linear non-degenerate, linear degenerate, non-linear non-degenerate and non-linear degenerate equation systems. For non-degenerate systems, inter-drag and diffusion terms are also considered to elucidate their effects on the solution stability. In these computations, the grid spacing is set as $\Delta x = 0.01$, which has been numerically verified to provide accurate numerical results if the solution remain stable. All computations are performed in the range of $-5 \leqslant x \leqslant 5$, which is shown to be large enough such that the imposed boundary conditions will not affect the resulting solutions in the interested region. For cases without diffusion term, the time step is chosen as the maximum Courant number based on the real part of complex eigenvalues being less than 0.5, $C_{\mathrm{R,max}} = 0.5$. For cases with diffusion term, an additional constraint on time step is introduced. This constraint is based on a dimensionless time step due to diffusion effect:

$$C_\mu = \frac{\mu \Delta t}{\Delta x^2}. \tag{51}$$

Therefore, the chosen time step is set to satisfy both the above constraint for the Courant number and that for the diffusion effect, $C_\mu \leqslant 0.3$. Grid convergence tests are also performed to investigate the effects of grid spacing on the solution accuracy.

Besides various equation types being solved, a variety of initial conditions, which includes the sinusoidal, exponential and hyperbolic tangent functions, are assigned. In the following paragraphs, the equations to be solved, initial conditions, available exact solutions and the resulting numerical results for these test problems will be subsequently described.

6.1. Linear non-degenerate system

The equation type to be solved in this category is given in Eq. (7a)–(7c) and its exact solution is shown in Eq. (8). In our calculations, the complex eigenvalue is chosen as

$$\lambda_R = 1.0 \quad \text{and} \quad \lambda_I = 0.5. \tag{52}$$

Three types of initial conditions at $t = 0$ are considered

$$\text{(i)} \qquad u_0(x) = 0, \quad v_0(x) = \cos(kx) \quad \text{with } k = 5\pi \text{ and } k = \pi, \tag{53a}$$

$$\text{(ii)} \qquad u_0(x) = 0, \quad v_0(x) = \cosh(kx) \quad \text{with } k = \pi/4, \tag{53b}$$

$$\text{(iii)} \qquad u_0(x) = 0, \quad v_0(x) = \tanh(kx) \quad \text{with } k = \pi/2. \tag{53c}$$

Condition (i) is a sinusoidal distribution, condition (ii) a exponential distribution and condition (iii) a hyperbolic tangent distribution. The corresponding exact solutions for the equation system and initial conditions are

$$\text{(i)} \qquad u(x,t) = \sinh(k\lambda_I t)\sin[k(x-\lambda_R t)], \quad v(x,t) = \cosh(k\lambda_I t)\cos[k(x-\lambda_R t)], \tag{54a}$$

$$\text{(ii)} \qquad u(x,t) = -\sin(k\lambda_I t)\sinh[k(x-\lambda_R t)], \quad v(x,t) = \cos(k\lambda_I t)\cosh[k(x-\lambda_R t)], \tag{54b}$$

$$\text{(iii)} \qquad u(x,t) = \frac{\sin(k\lambda_I t)\cos(k\lambda_I t)}{\sinh^2[k(x-\lambda_R t)] + \cos^2(k\lambda_I t)}, \quad v(x,t) = \frac{\sinh[k(x-\lambda_R t)]\cosh[k(x-\lambda_R t)]}{\sinh^2[k(x-\lambda_R t)] + \cos^2(k\lambda_I t)}. \tag{54c}$$

Fig. 1(a) demonstrates the calculation results for initial condition (i) and $k = 5\pi$ at $t = 0.5$ with first-order upwind scheme (17a). Corresponding exact solution is also included in this figure for comparison. From Fig. 1(a), it is shown that the computational result will increase indefinitely and, however, its growth rate is less than that of exact solution. In this sense, the numerical scheme can be regarded as a stable scheme. Meanwhile, significant diffusive effects for the numerical scheme are also observed in this figure. These phenomena are coincident with the previous normal-mode analysis for the differential and difference equations. Results with second-order accurate Fromm scheme (17d) for this problem is depicted in Fig. 1(b). Compared with first-order scheme, the Fromm scheme provides more accurate results as in the simulations of hyperbolic equation systems. For smaller wave number with $k = \pi$, Fig. 2(a) shows the computational results with Fromm scheme at $t = 0.5$, which is in agreement with the exact solution. However, as time increases, high frequency error inherent in the calculation will grow and finally overwhelm the useful information. These phenomena can be observed in Figs. 2(b) and (c) for $t = 0.775$ and $t = 0.8$, respectively. In general, it is quite difficult to completely eliminate this spurious artifact for a numerical scheme to simulate

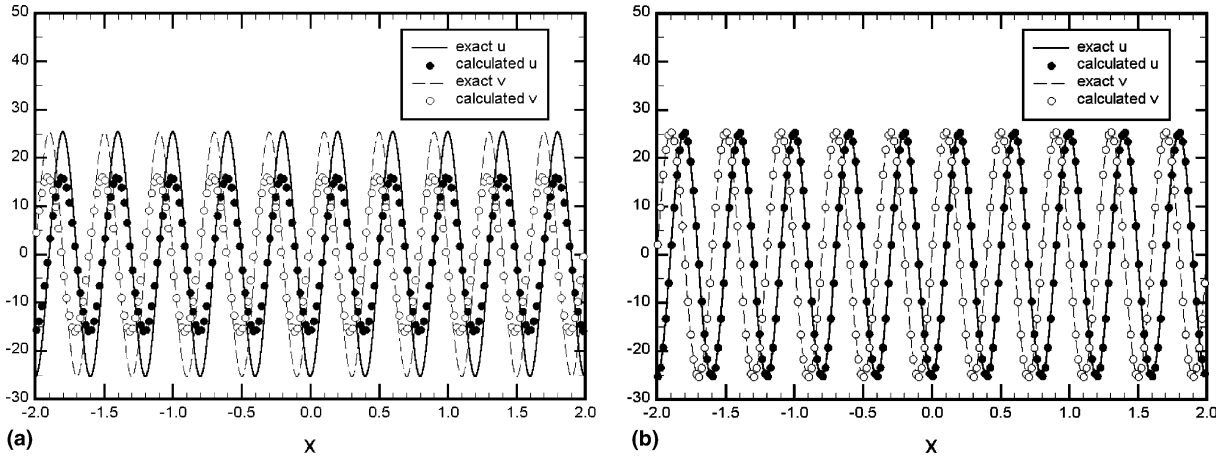

Fig. 1. Computational results for linear non-degenerate system with initial condition (i) and $k = 5\pi$ at $t = 0.5$: (a) the first-order scheme, (b) the Fromm scheme.

an ill-posed problem. For problems of initial condition (ii) and initial condition (iii), Figs. 3 and 4 show the computational results compared with exact solutions at $t = 1.0$. These results are obtained by the Fromm scheme. As shown in these figures, the proposed scheme can accurately simulate non-degenerate equation system if the useful information is not significantly polluted by the high frequency errors. To investigate the effects of grid spacing on the solution accuracy and demonstrate the characteristics of the numerical solution for the non-hyperbolic system, we define the error measure for the calculated result

$$E_n = \left\{ \left[\sum_{i=i_S}^{i_E} (u_{E,i} - u_{C,i})^2 + (v_{E,i} - v_{C,i})^2 \right] \Big/ (i_E - i_S + 1) \right\}^{1/2}, \tag{55}$$

where i_S and i_E are the starting and ending nodal indexes in the interested domain ($-2 \leqslant x \leqslant 2$), respectively. Subscripts E and C, respectively, denote the exact and calculated solutions. Fig. 5(a) illustrates the effects of grid spacing on the solution accuracy obtained by 1UD and Fromm schemes for problem of initial condition (i) and $k = \pi$ at $t = 0.5$. These results are obtained with a constant maximum Courant number based on the real part of complex eigenvalues, $C_{R,max} = 0.5$. It is clearly shown that as Δx decreases from the coarse spacing ($\Delta x = 0.1$), the solution error will first decrease, then reach a minimum value, and finally increase rapidly to depict a polluted solution. This is the general scenario of a numerical solution for an unstable non-hyperbolic system [11]. That is, for a given evolution time, there is a grid spacing constraint to avoid a contaminated solution. Meanwhile, Fig. 5(a) also illustrates the Fromm and 1UD schemes will, respectively, provide second-order and first-order accurate solutions if the solution has not been overwhelmed by the high-frequency error. Evolutions of solution errors for this case with $\Delta x = 0.01$ are shown in Fig. 5(b). From this figure, one can observe that the solution error will mildly increase if the calculated solution has not been polluted. However, after a certain time, the solution error will increase dramatically which implies the solution has been contaminated by the high-frequency error. This critical time can be estimated from the information growth rate indicated in the amplification matrix of a difference scheme (24a)–(24c) and (28). Let λ_k be the amplification factor of a specific wave-number, k, and define the maximum information growth rate,

$$\lambda_{max} = \operatorname*{Max}_{|k\Delta x| \leqslant \pi} \lambda_k. \tag{56a}$$

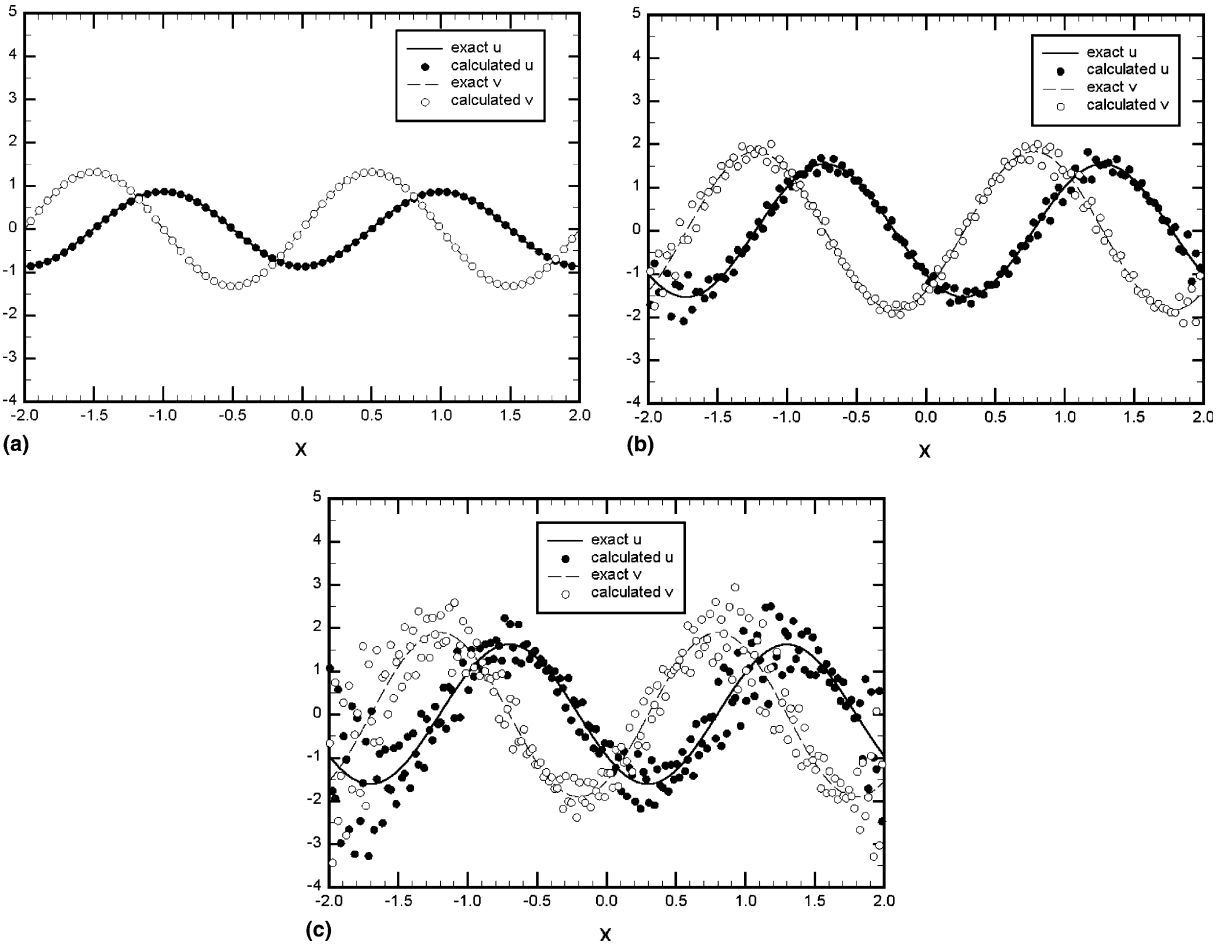

Fig. 2. Computational results for linear non-degenerate system with initial condition (i) and $k = \pi$ by the Fromm scheme: (a) $t = 0.5$, (b) $t = 0.775$, (c) $t = 0.8$.

Since the amplitude of disturbance existing in the initial condition can be assumed to be equal to machine rounding error, $10^{-\varepsilon}$, the critical time, τ, at which the disturbance shows a comparable amount as the useful information can be estimated to satisfy the following relation:

$$10^{-\varepsilon} \approx \left(\frac{\lambda_k}{\lambda_{\max}}\right)^{\tau/\Delta t} \tag{56b}$$

or

$$\tau \approx \varepsilon \Delta t / \log(\lambda_{\max}/\lambda_k). \tag{56c}$$

In the present example with assigned computational parameters ($k = \pi$, $\Delta x = 0.01$, $C_R = 0.5$ and $C_I = 0.25$), the information growth rates for 1UD (24a)–(24c) and Fromm (28) schemes can be obtained from direct numerical evaluations

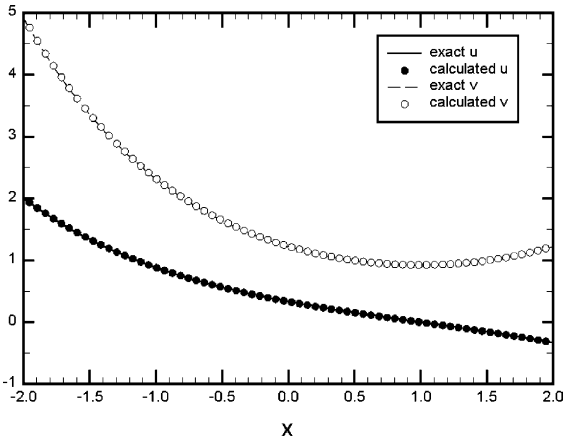

Fig. 3. Computational results for linear non-degenerate system with initial condition (ii) at $t = 1.0$ by the first-order scheme.

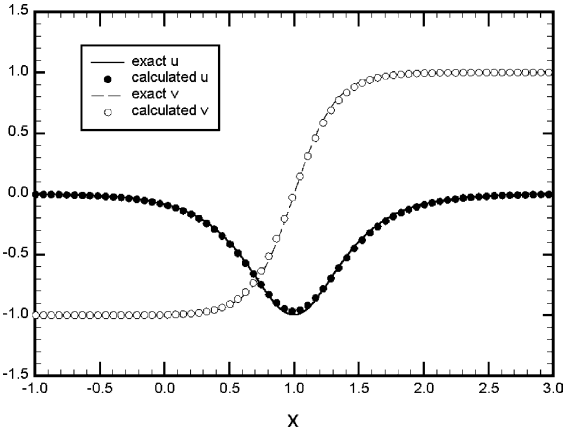

Fig. 4. Computational results for linear non-degenerate system with initial condition (iii) at $t = 1.0$ by the first-order scheme.

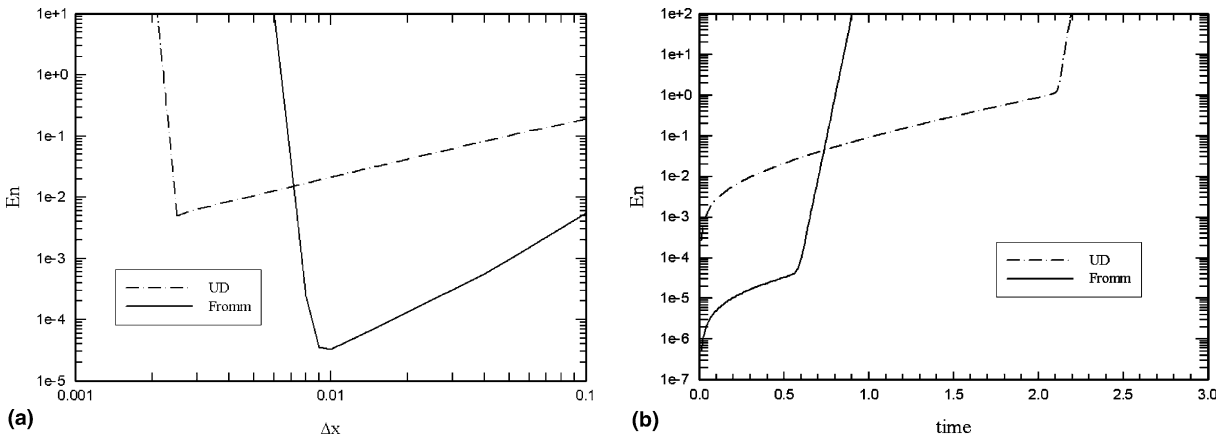

Fig. 5. Solution error for linear non-degenerate system with initial condition (i) and $k = \pi$: (a) effect of grid spacing at $t = 1.0$, (b) time evolution with $\Delta x = 0.01$.

$$\left(\frac{\lambda_{\max}}{\lambda_k}\right)_{1\mathrm{UD}} = 1.0946 \quad \text{and} \quad \left(\frac{\lambda_{\max}}{\lambda_k}\right)_{\mathrm{Fromm}} = 1.2656 \tag{57a}$$

and the corresponding critical times for the present machine rounding error ($\varepsilon = 16$) are

$$\tau_{1\mathrm{UD}} \approx 2.037 \quad \text{and} \quad \tau_{\mathrm{Fromm}} \approx 0.782. \tag{57b}$$

These critical times are in very agreement with those depicted in Fig. 5(b) ($E_n = 1$). For comparison, the critical time for the differential system can also be estimated from amplification factor in Eq. (22)

$$\tau_{\mathrm{diff}} \approx 2.3025\varepsilon/\lambda_{\mathrm{I}}/(\pi/\Delta x - k) = 0.2369, \tag{57c}$$

which is less than those for 1UD and Fromm schemes.

6.2. Linear degenerate system

The equation type to be solved in this category is listed in Eq. (34) and its exact solution can be derived from Eq. (35). Eigenvalue for the present calculations is set to be $\lambda = 1.0$. Various initial conditions as in Eq. (53) are assigned and their corresponding exact solutions are

$$\text{(i)} \qquad u(x,t) = tk\sin[k(x-\lambda t)], \quad v(x,t) = \cos[k(x-\lambda t)], \tag{58a}$$

$$\text{(ii)} \qquad u(x,t) = -tk\sinh[k(x-\lambda t)], \quad v(x,t) = \cosh[k(x-\lambda t)], \tag{58b}$$

$$\text{(iii)} \qquad u(x,t) = -tk\,\mathrm{sech}^2[k(x-\lambda t)], \quad v(x,t) = \tanh[k(x-\lambda t)]. \tag{58c}$$

Since the equation system is degenerate and its eigenvalue is not a complex number, the increasing rate of information is linearly proportional to the wave number. As compared with the exponential growth rate in previous non-degenerate system, the high frequency error inherent in this degenerate system will not severely influence the useful information if the following condition is satisfied:

$$10^{-\varepsilon}\frac{\pi}{\Delta x} \ll k. \tag{59}$$

Figs. 6(a) and (b) illustrate the computational results for the initial condition (i) with $k = 5\pi$ at $t = 0.5$ and with $k = \pi$ at $t = 1.0$, respectively. Figs. 7 and 8, respectively, depict the computational results for condition (ii) and condition (iii) at $t = 1.0$. These computations are performed with the Fromm scheme. From these calculations, it is shown that the proposed scheme can provide numerical results in agreement with exact solutions for the linear degenerate system.

6.3. Non-linear non-degenerate system

The equation type to be solved in this category is chosen as

$$\frac{\partial u}{\partial t} + u\frac{\partial u}{\partial x} - v\frac{\partial v}{\partial x} = 0, \tag{60a}$$

$$\frac{\partial v}{\partial t} + v\frac{\partial u}{\partial x} + u\frac{\partial v}{\partial x} = 0. \tag{60b}$$

This is also a conservative non-linear system. If we introduce a complex variable

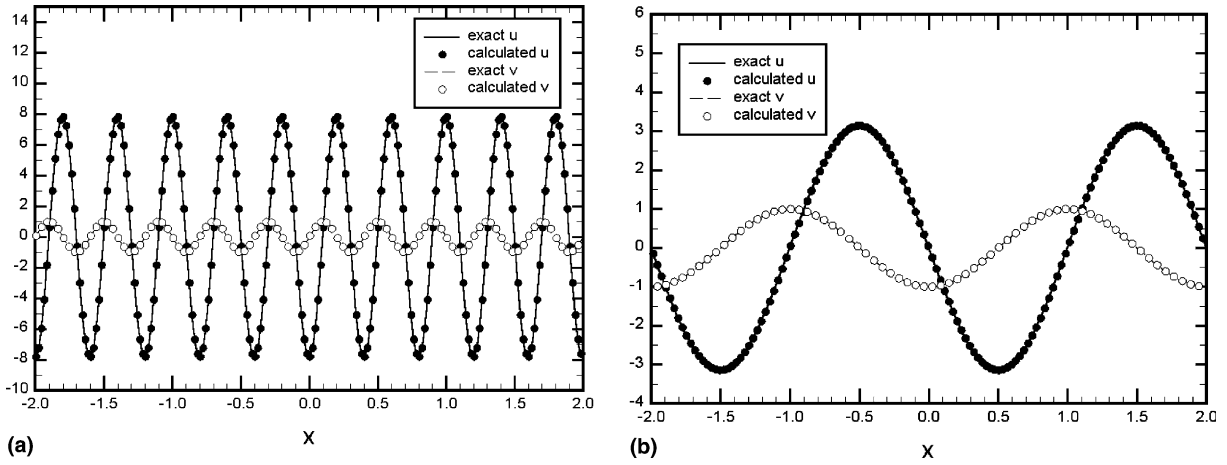

Fig. 6. Computational results for linear degenerate system with initial condition (i) by the Fromm scheme: (a) $k = 5\pi$ at $t = 0.5$, (b) $k = \pi$ at $t = 1.0$.

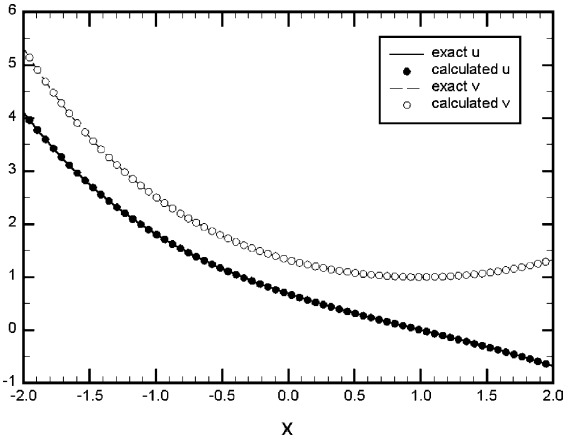

Fig. 7. Computational results for linear degenerate system with initial condition (ii) at $t = 1.0$ by the Fromm scheme.

$$\omega = u + \mathrm{j}v, \tag{61}$$

then the above equation system (60) can be rearranged as

$$\frac{\partial \omega}{\partial t} + \omega \frac{\partial \omega}{\partial x} = 0. \tag{62}$$

As compared with the Burgers' equation in real space, this equation system can be designated as the complex Burgers' equation with eigenvaules

$$\lambda_1 = u + \mathrm{j}v \quad \text{and} \quad \lambda_2 = u - \mathrm{j}v. \tag{63}$$

The exact solution for a general smooth initial condition (7c) at any particular location (x, t) can be obtained by the following relation:

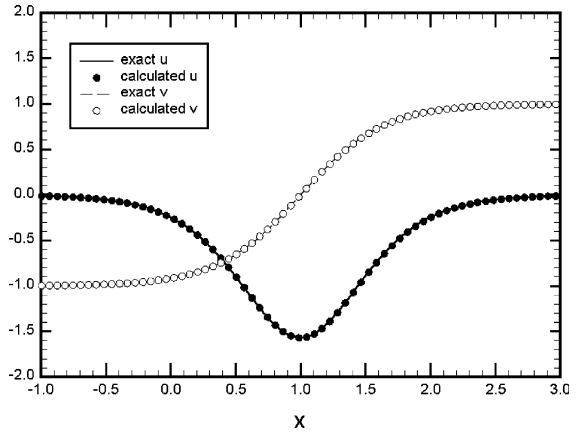

Fig. 8. Computational results for linear degenerate system with initial condition (iii) at $t = 1.0$ by the Fromm scheme.

$$f_u + \mathrm{j}f_v = u + \mathrm{j}v - u_0(x - ut - \mathrm{j}vt) - \mathrm{j}v_0(x - ut - \mathrm{j}vt) = 0. \tag{64}$$

Therefore, the exact solution can be found with a suitable iterative method. For the three types of initial conditions given in Eq. (53a)–(53c), the corresponding exact solutions will satisfy the following relation:

$$\text{(i)} \qquad f_u = u + \sinh(kvt)\sin[k(x - ut)] = 0, \quad f_v = v - \cosh(kvt)\cos[k(x - ut)] = 0, \tag{65a}$$

$$\text{(ii)} \qquad f_u = u - \sin(kvt)\sinh[k(x - ut)] = 0, \quad f_v = v - \cos(kvt)\cosh[k(x - ut)] = 0, \tag{65b}$$

$$\text{(iii)} \qquad f_u = u + \frac{\sin(kvt)\cos(kvt)}{\sinh^2[k(x - ut)] + \cos^2(kvt)} = 0, \quad f_v = v - \frac{\sinh[k(x - ut)]\cosh[k(x - ut)]}{\sinh^2[k(x - ut)] + \cos^2(kvt)} = 0. \tag{65c}$$

For comparison with numerical results, we adopted the Newton–Raphson method to iteratively find the exact solution satisfying the following convergence criteria between two successive calculations:

$$\max(|\Delta u|, |\Delta v|) \leqslant 10^{-7} \quad \text{and} \quad \max(|f_u|, |f_v|) \leqslant 10^{-10}. \tag{66}$$

Further reduction on the convergence criteria will not increase the solution accuracy significantly in the present calculations. The coefficient matrix between the right and left states in our scheme (20) is chosen to satisfy the general jump condition (20d)

$$\bar{\mathbf{A}}(\mathbf{U}_\mathrm{R}, \mathbf{U}_\mathrm{L}) = \mathbf{A}\left(\frac{\mathbf{U}_\mathrm{R} + \mathbf{U}_\mathrm{L}}{2}\right) = \frac{1}{2}\begin{pmatrix} (u_\mathrm{R} + u_\mathrm{L}) & -(v_\mathrm{R} + v_\mathrm{L}) \\ (v_\mathrm{R} + v_\mathrm{L}) & (u_\mathrm{R} + u_\mathrm{L}) \end{pmatrix}. \tag{67}$$

From the previous experience in calculating linear non-degenerate system, more severe numerical stability problem due to the high frequency error can be expected in these simulations. Meanwhile, besides this high frequency error in the computations, another numerical difficult may be encountered due to the oscillatory solutions originating from the computational boundaries. These oscillatory solutions will grow indefinitely such that the eigenvalues near the computational boundaries will approach infinity. Therefore, the chosen time step to yield a stable solution in the interested domain will become too small to proceed to further practical computations. Figs. 9(a) and (b) illustrate the computational results for the initial condition (i) with $k = 5\pi$ at $t = 0.04$ and with $k = \pi$ at $t = 0.08$, respectively. Figs. 10 and 11, respectively, depict the calculated results for the condition (ii) at $t = 0.03$ and for the condition (iii) at $t = 0.2$. These computational

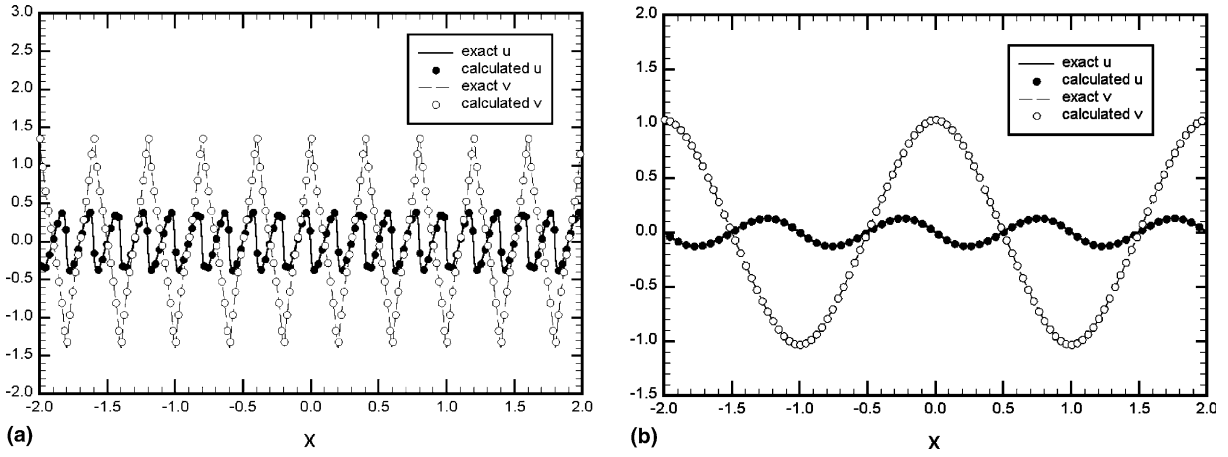

Fig. 9. Computational results for non-linear nondegenerate system with initial condition (i) by the Fromm scheme: (a) $k = 5\pi$ at $t = 0.04$, (b) $k = \pi$ at $t = 0.08$.

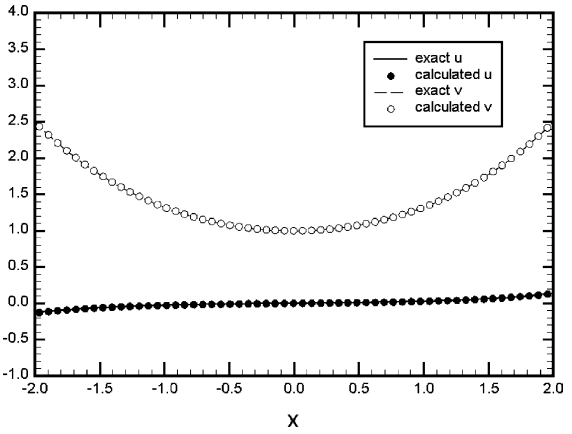

Fig. 10. Computational results for non-linear non-degenerate system with initial condition (ii) at $t = 0.03$ by the first-order scheme.

results are obtained by the Fromm scheme. At these limited available simulation time, the computational results are in agreement with the exact solution.

6.4. Non-linear degenerate system

The equation type to be solved in this category is chosen as:

$$\frac{\partial u}{\partial t} + v\frac{\partial u}{\partial x} + u\frac{\partial v}{\partial x} = 0, \tag{68a}$$

$$\frac{\partial v}{\partial t} + v\frac{\partial v}{\partial x} = 0, \tag{68b}$$

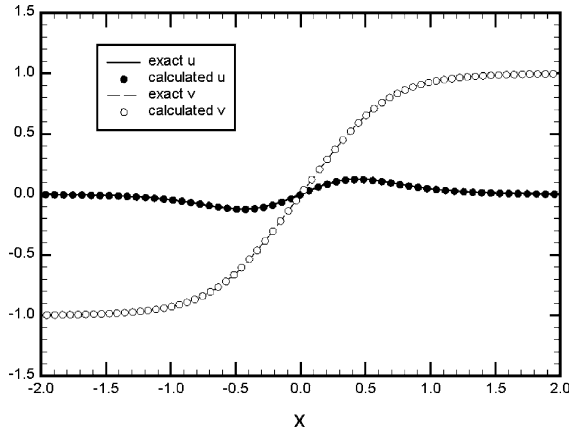

Fig. 11. Computational results for non-linear non-degenerate system with initial condition (iii) at $t = 0.2$ by the first-order scheme.

where the second equation is the conventional Burgers' equation. Eigenvalues for this conservative non-linear system are

$$\lambda_1 = \lambda_2 = v. \tag{69}$$

The exact solution for the general initial condition (7c) can then be found from the following relations:

$$u = \frac{u_0(x - vt)}{1 + tv_0'(x - vt)}, \tag{70a}$$

$$f_v = v - v_0(x - vt) = 0. \tag{70b}$$

It needs a suitable iterative method to solve Eq. (70b) for v, which is then substituted into Eq. (70a) to obtain the solution for u. For the initial condition given in Eq. (53), $u_0(x)$ is modified to obtain a non-trivial distribution of $u(x, t)$

$$u_0(x) = 1.0. \tag{71}$$

The corresponding exact solutions will satisfy the following relations:

$$\text{(i)} \qquad u = \frac{1}{1 - tk\sin[k(x - vt)]}, \quad f_v = v - \cos[k(x - vt)] = 0, \tag{72a}$$

$$\text{(ii)} \qquad u = \frac{1}{1 + tk\sinh[k(x - vt)]}, \quad f_v = v - \cosh[k(x - vt)] = 0, \tag{72b}$$

$$\text{(iii)} \qquad u = \frac{1}{1 + tk\,\mathrm{sech}^2[k(x - vt)]}, \quad f_v = v - \tanh[k(x - vt)] = 0. \tag{72c}$$

Newton–Raphson method is adopted to iteratively solve for the equation, $f_v = 0$, until the convergence criteria between two successive calculations has been satisfied

$$|\Delta v| \leqslant 10^{-7} \quad \text{and} \quad |f_v| \leqslant 10^{-10}. \tag{73}$$

Figs. 12(a) and (b) illustrate the computational results for the initial condition (i) with $k = 5\pi$ at $t = 0.05$ and with $k = \pi$ at $t = 0.3$, respectively. Figs. 13 and 14(a), respectively, depict the calculated results for the condition (ii) at $t = 0.04$ and for the condition (iii) at $t = 1.0$. These computational results are obtained by the Fromm scheme. Quite satisfactory results are obtained as compared with the exact solutions. Fig. 14(b) shows the computational result for the hyperbolic tangent initial condition (iii) with the first-order upwind scheme. A phenomenon similar to the sonic-point deficiency in the calculation of hyperbolic system can be observed near $x = 0$ [19]. Meanwhile, the first-order upwind scheme provides more diffusive solution as compared with the Fromm scheme.

6.5. Non-degenerate system with inter-drag and diffusion terms

As evident in the previous calculations, the pure non-hyperbolic system will yield an ill-posed problem. Calculated solutions will be contaminated by the high frequency errors. However, such an ill-posed system

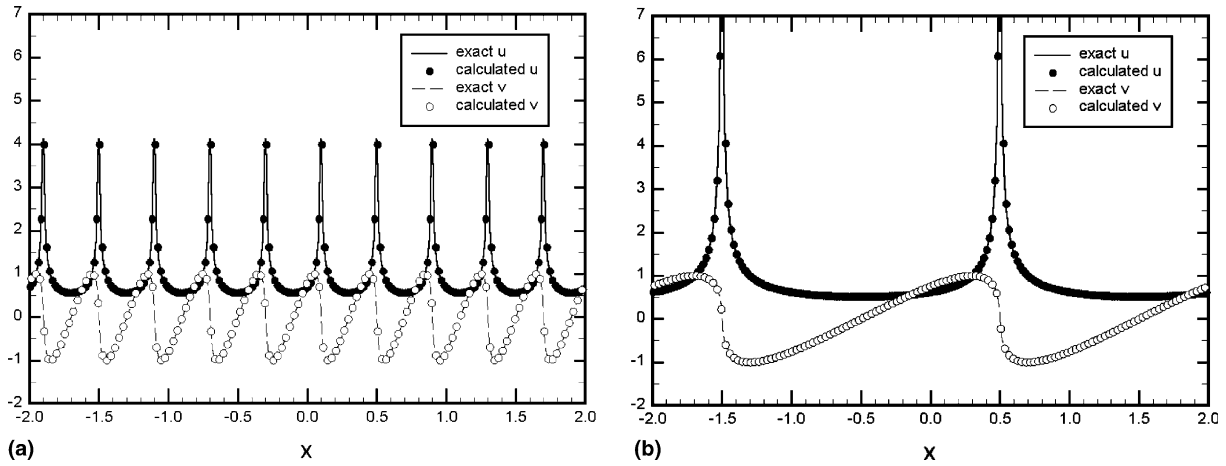

Fig. 12. Computational results for non-linear degenerate system with initial condition (i) by the Fromm scheme: (a) $k = 5\pi$ at $t = 0.05$, (b) $k = \pi$ at $t = 0.3$.

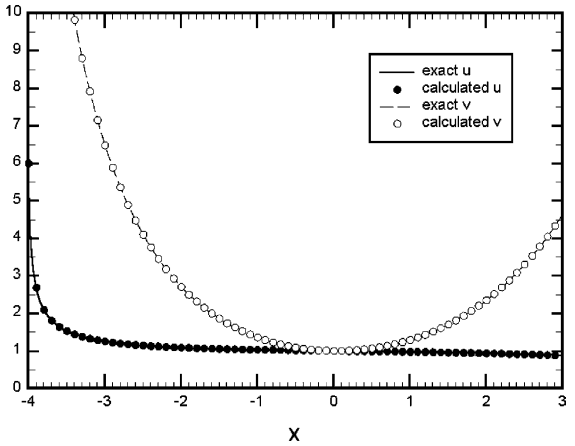

Fig. 13. Computational results for non-linear degenerate system with initial condition (ii) at $t = 0.04$ by the Fromm scheme.

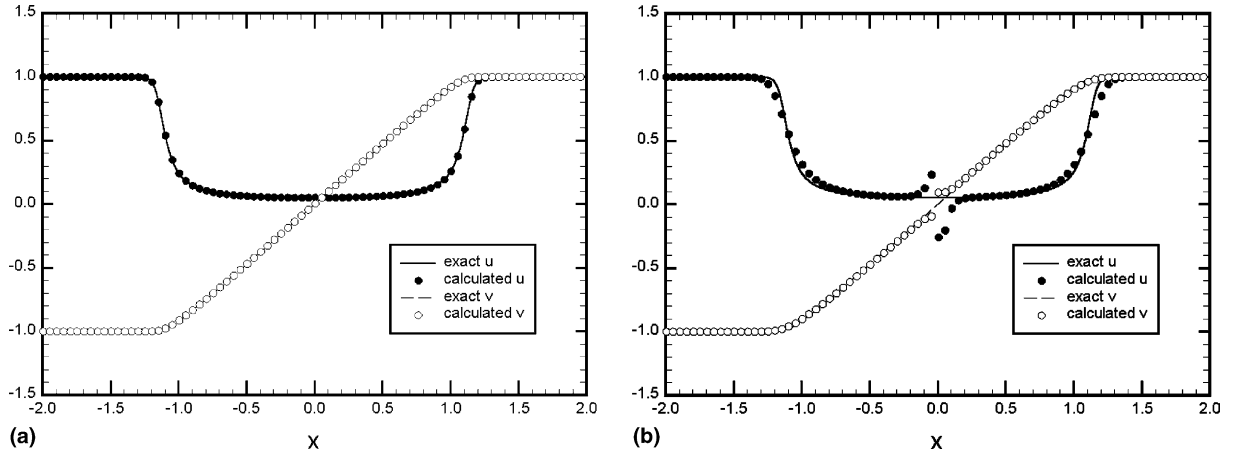

Fig. 14. Computational results for non-linear degenerate system with initial condition (iii) with $k = 6\pi$ at $t = 1.0$: (a) the Fromm scheme, (b) the first-order scheme.

can be stabilized by additional inter-drag and diffusion terms. In this section, we will perform numerical evidence to show the usefulness of proposed scheme by solving both linear and non-linear problems. First, a linear system is simulated and the calculated result will be compared with the available exact solution. In this calculation, the adopted inter-drag and diffusion coefficients are set to be $\mu = 0.01$ and $f_d = \lambda_I^2/2\mu$, respectively, to guarantee a stable solution (43b). The initial condition is assigned the sinusoidal distribution as in Eq. (53a) and the corresponding exact solution will be

$$u = \frac{1}{2}[\exp(-\tilde{\lambda}_2) - \exp(-\tilde{\lambda}_1)]\frac{f_d \cos[k(x - \lambda_R t)] + k\lambda_I \sin[k(x - \lambda_R t)]}{\sqrt{f_d^2 + k^2\lambda_I^2}}, \tag{74a}$$

$$v = \frac{1}{2}[\exp(-\tilde{\lambda}_2) + \exp(-\tilde{\lambda}_1)]\cos[k(x - \lambda_R t)] \tag{74b}$$

with the eigenvalues, $\tilde{\lambda}_1$ and $\tilde{\lambda}_2$, given in (41a), (41b). The calculated results by the Fromm scheme for the higher wave number with $k = 5\pi$ at $t = 0.5$ and for the lower wave number with $k = \pi$ at $t = 1.0$ are, respectively, illustrated in Figs. 15(a) and (b). Effects of grid spacing on solution accuracy at $t = 1.0$ for $k = \pi$ and the evolution of solution accuracy with $\Delta x = 0.01$ are shown in Figs. 16(a) and (b), respectively. Definition of solution error measure (E_n) has been given in Eq. (55). In these figures, it is clearly shown that the spurious artifact due to high frequency disturbance is eliminated and the proposed methodology with Fromm scheme may provide second-order accurate numerical solution for the stable non-hyperbolic system. Furthermore, we apply the proposed scheme to solve a non-linear system,

$$\frac{\partial u}{\partial t} + u\frac{\partial u}{\partial x} - v\frac{\partial v}{\partial x} + C_D|u - v|(u - v) - \mu\frac{\partial^2 u}{\partial x^2} = 0, \tag{75a}$$

$$\frac{\partial v}{\partial t} + v\frac{\partial u}{\partial x} + u\frac{\partial v}{\partial x} + C_D|u - v|(v - u) - \mu\frac{\partial^2 v}{\partial x^2} = 0. \tag{75b}$$

This equation system can be regarded as a simplified two-phase model equation, where u and v are the phasic velocities and C_D the inter-phase drag coefficient. The eigenvalues for this system are $\lambda_1 = u - jv$ and

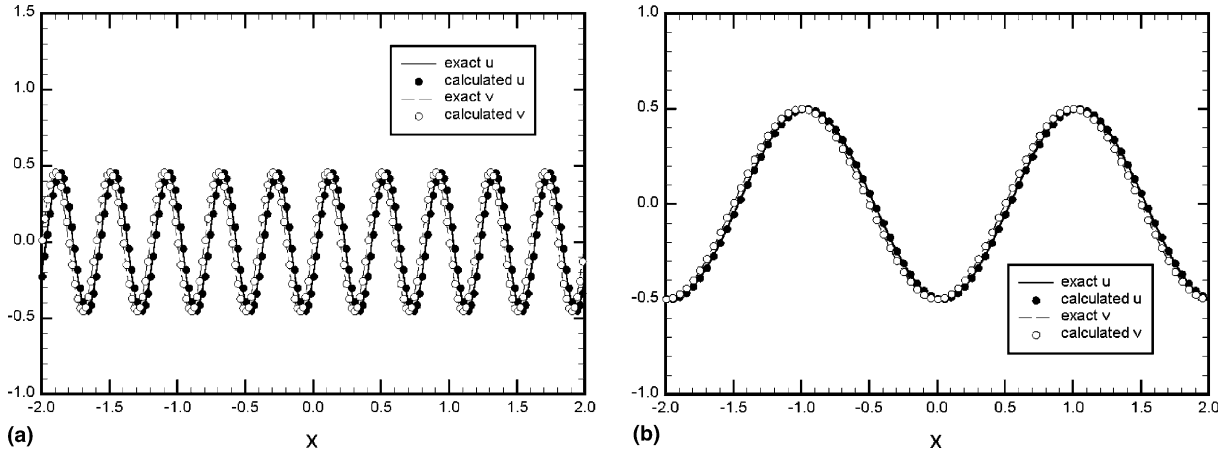

Fig. 15. Computational results for linear non-degenerate system with inter-drag and diffusion terms for initial condition (i) by the Fromm scheme: (a) $k = 5\pi$ at $t = 0.5$, (b) $k = \pi$ at $t = 1.0$.

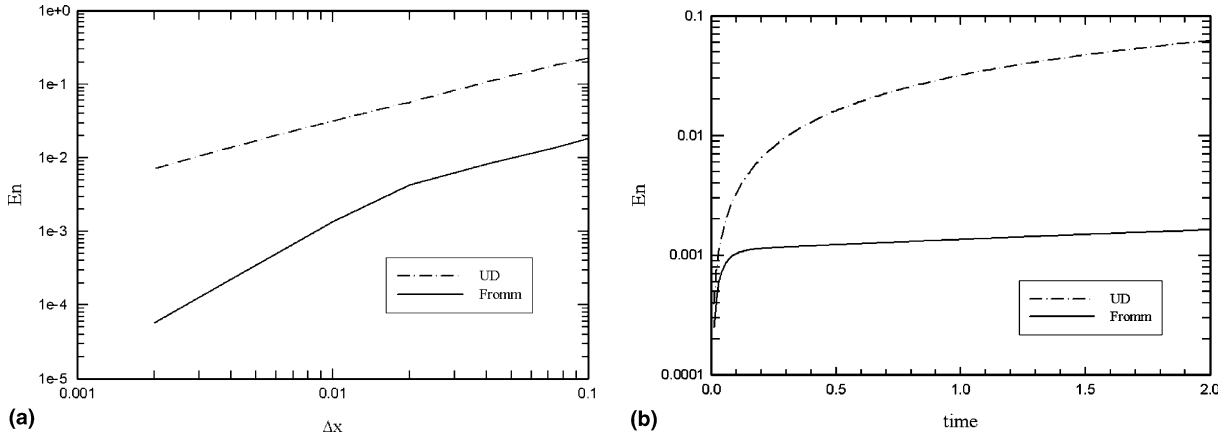

Fig. 16. Solution error for linear non-degenerate system with inter-drag and diffusion terms for initial condition (i) and $k = \pi$: (a) effect of grid spacing at $t = 1.0$, (b) time evolution with $\Delta x = 0.01$.

$\lambda_2 = u + \mathrm{j}v$. As the stability condition for linear system shown in Eq. (43b), the corresponding condition for this model equation is

$$C_{\mathrm{D}}\mu|u - v| \geqslant v^2/2. \tag{76}$$

That is, for small phasic velocity difference ($|u - v|$), this is an unstable system and the phasic velocities will grow; while for large phasic velocity difference, this system may be stabilized with the diffusion and inter-drag terms. With a certain appropriate initial condition, one may expect to observe the magnitude of phasic velocities grow in initial stage and diminish in a later stage. This equation system consists of many essential ingredients to simulate the non-linear non-hyperbolic system of equations. In the present calculation, the diffusion and drag coefficients are, respectively, assigned as $\mu = 0.05$ and $C_{\mathrm{D}} = 0.5$. Initial condition is set as given in Eq. (53a) for a sinusoidal distribution with $k = \pi$. Since it is impossible to obtain the exact solution

for this problem, the computational results are shown to depict the interactions between phasic velocities and effects of inter-drag and diffusion terms. The calculation is performed with the second-order Fromm scheme.

For comparison, the initial distributions of solution vectors, u and v, are shown in Fig. 17(a). Since the resulting solutions are periodic functions, the following discussions can be confined in the range of $-1 < x \leqslant 1$. At initial stage, effects of viscous term can be neglected as compared with the inter-convective term, $v(\partial v/\partial x)$ in Eq. (75a) and inter-drag term. Therefore, as shown in Fig. 17(b) for $t = 0.25$, the distributions of u and v can be, respectively, approximated by the following relations:

(i) for $|x| \leqslant 0.5$

$$u \approx -tk\cos(kx)\sin(kx) + C_{\mathrm{D}} t\cos^2(kx),$$

$$v \approx \cos(kx) - C_{\mathrm{D}}\cos^2(kx),$$

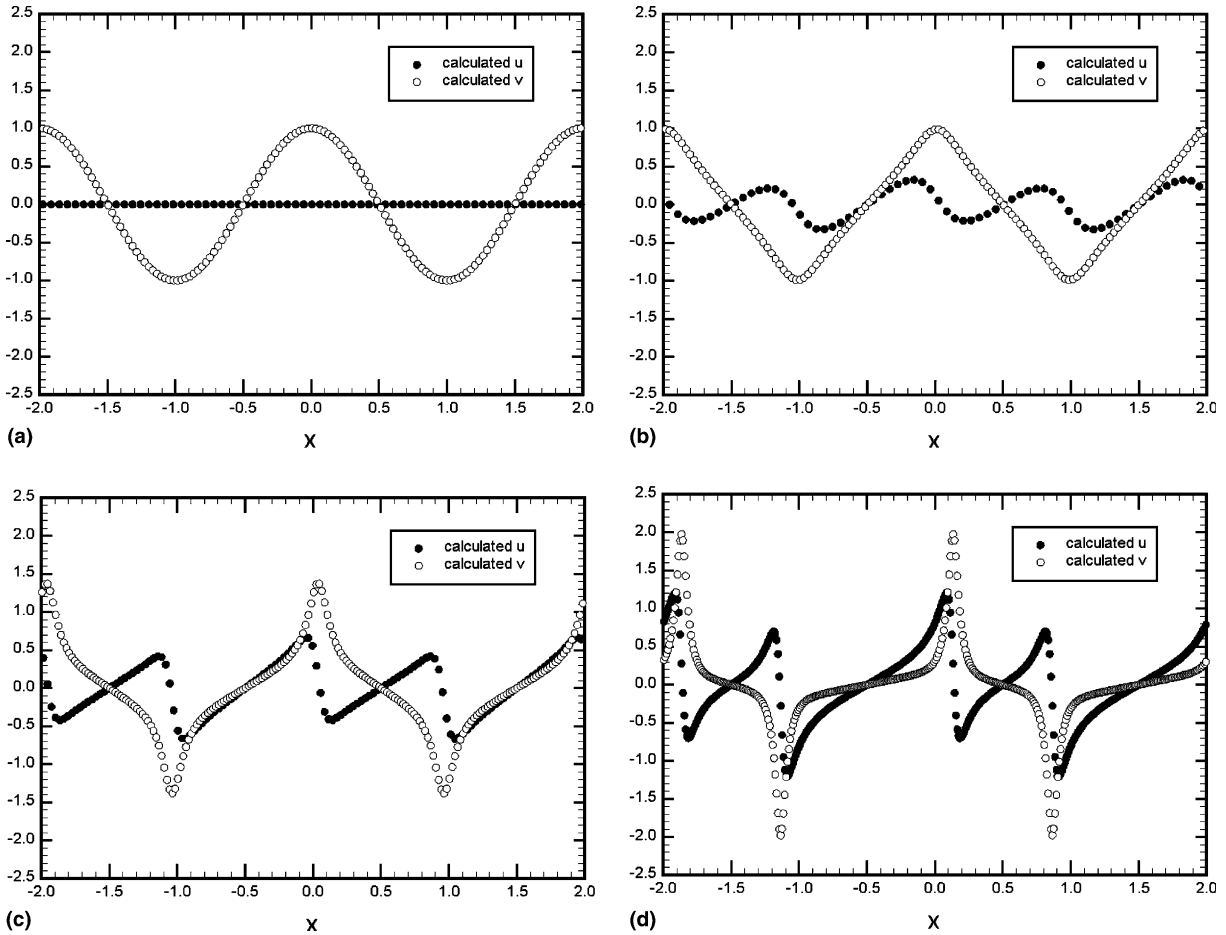

Fig. 17. Computational results for non-linear non-degenerate system with inter-drag and diffusion terms for initial condition (i) and by the Fromm scheme: (a) $t = 0$, (b) $t = 0.25$, (c) $t = 0.5$, (d) $t = 1.0$, (e) $t = 1.5$, (f) $t = 2.0$, (g) $t = 3.0$, (h) $t = 4.0$.

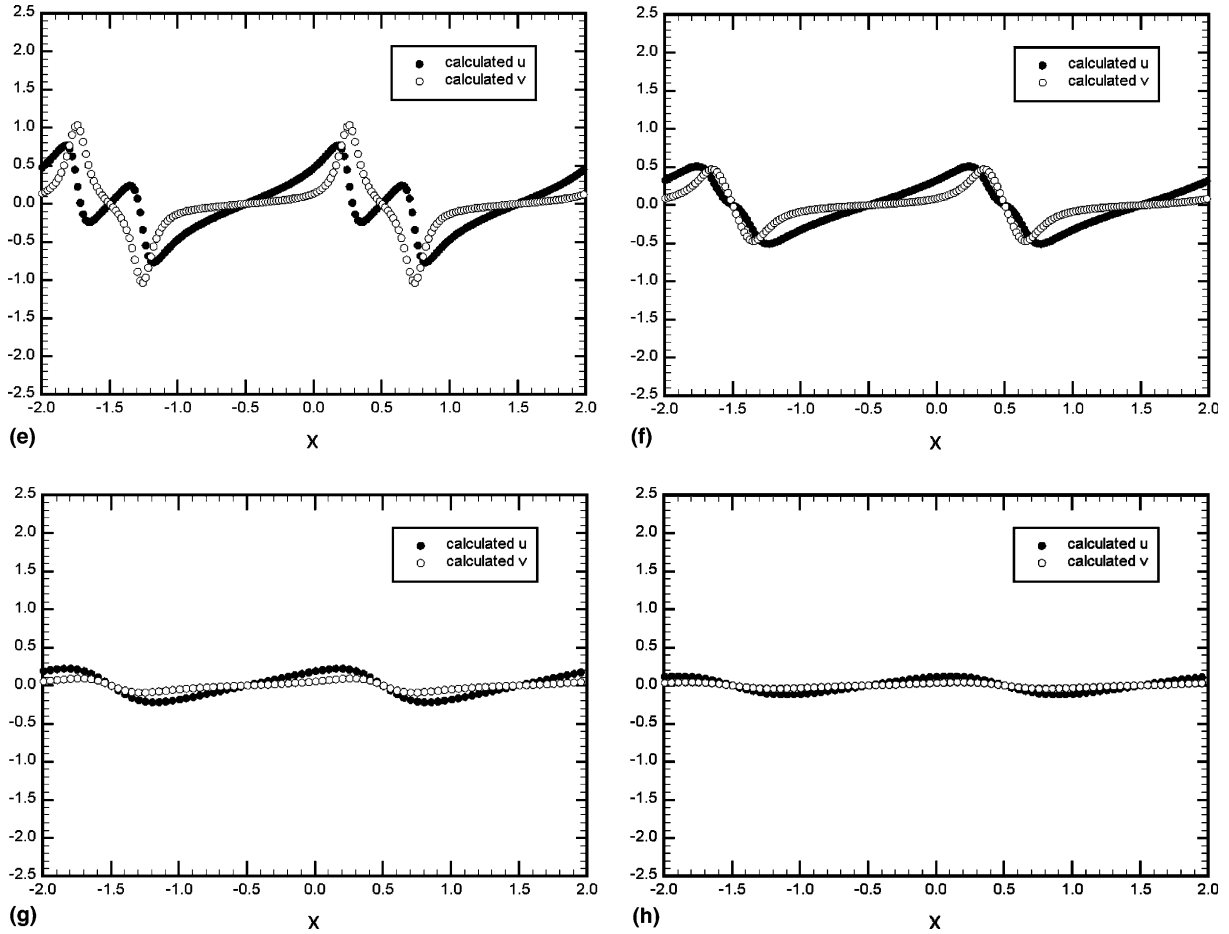

Fig. 17. (*continued*)

(ii) for $|x| > 0.5$

$$u \approx -tk\cos(kx)\sin(kx) - C_{\mathrm{D}}t\cos^2(kx),$$

$$v \approx \cos(kx) + C_{\mathrm{D}}\cos^2(kx)$$

if the propagation terms, $u(\partial u/\partial x)$ in Eq. (75a) and $u(\partial v/\partial x)$ in Eq. (75b), are also neglected for small u. As time evolves, effects of propagation terms will affect the solution vectors to form a N-wave type for u, which forms steep gradients around at $x = 0$ and $x = 1$. Such steep gradients of u will further increase the magnitude of v through the inter-convective term, $v(\partial u/\partial x)$. Therefore, spikes of v occur around the steep gradient of u. Such phenomena are clearly illustrated in Fig. 17(c) for $t = 0.5$. Further interaction between phasic velocities will further enforce the magnitudes of spikes in v and gradients in u. Meanwhile, the inter-drag term will decrease the difference between phasic velocities ($C_{\mathrm{D}} > 0$). The magnitude of u near $x = 0$ will be subsequently increased and near $x = 1$ decreased. With this effect, the steep gradient at $x = 0$ will propagate in the positive x-direction and that at $x = 1$ in the negative direction. This is the scenario observed in Fig. 17(d) for $t = 1.0$. As time further increases, the effects of diffusion term will dominate the

distributions of solution vectors near steep gradients and subsequently decrease the magnifying effects due to inter-convective terms. This phenomenon can be observed in Fig. 17(e) for $t = 1.5$. As can be seen in Fig. 17(f) for $t = 2.0$, the two steep gradients of u originated at $x = 0$ and $x = 1$ merge; whereas, the gradient of u and magnitudes of v around these gradients decrease. Finally, all information will diminish due to the inter-drag and diffusion effects as illustrated Fig. 17(g) for $t = 3.0$ and Fig. 17(h) for $t = 4.0$. From above observations, it is evident that the computational results can be reasonably interpreted by the non-linear interactions between solution vectors.

7. Conclusions

Although the characteristic form of a non-hyperbolic equation system will consist of complex quantities, it can be transformed into an associated canonical form in real space. This procedure is detailed in the present study by introducing an appropriate eigensystem transformation. Based on the canonical expression, a general second-order scheme can be constructed to simulate the equation system. This scheme is coincident with the well-established upwind scheme if the equation system becomes hyperbolic. To justify our proposition, numerical analyses are performed to show the deficiency of the segregated treatment for coupled equations, which may consequently yield unstable solution for a simple linear hyperbolic system. Meanwhile, normal-mode analysis is also employed to indicate the stability of the proposed scheme and the associated time step constraint. The proposed scheme is also extended to solve degenerate equation systems. Effects of inter-drag and diffusion terms to stabilize the non-hyperbolic system are also investigated. Several representative model equations are solved to verify the feasibility of the present scheme. Pure non-hyperbolic systems are solved and compared with the available exact solutions. Since these systems may form ill-posed problems, the solutions will be eventually contaminated by the high frequency errors inherent in the numerical calculations. However, accurate results can be obtained with the present method before the high frequency errors dominate the solution information. For degenerate systems with real eigenvalues, the computational results are in very agreement with the exact solutions since the high frequency error will not pollute the useful information. Numerical results also show that additional inter-drag and diffusion terms may stabilize the non-hyperbolic system. Accurate results are obtained for the model linear problem. As for the non-linear case, a model two-phase equation system is simulated by the proposed scheme. All computational results can be reasonably interpreted by the interactions between phasic velocities. Therefore, based on the numerical analyses and computational experiments, one can conclude that the present scheme may be a useful tool to solve the general system of equations without regard to their hyperbolcity. Therefore, subsequent study will be conducted to incorporate the present method with the algebraic eigensystem expressions for model two-fluid equations to provide an efficient and accurate simulation tool for the two-phase flow problems.

References

[1] M.Y. Hussaini, B. Van Leer, J.R. Van Rosendale (Eds.), Upwind and High-Resolution Schemes, Springer, Berlin, 1997.
[2] I. Toumi, A. Kumaro, An approximate linearized Riemann solver for a two-fluid model, Journal of Computational Physics 124 (1997) 286–300.
[3] I. Tiselj, S. Petelin, Modelling of two-phase flow with second-order accurate schemes, Journal of Computational Physics 136 (1997) 503–521.
[4] Y.H. Hwang, W.J. Wu, N.M. Chung, Algebraic eigensystem expressions for the two-phase flow computations, in: Proceedings of 7th National Conference on Computational Fluid Dynamics, D9-D14, 2000.
[5] M.C. No, M.S. Kazimi, Effects of virtual mass on the mathematical characteristics and numerical stability of the two-fluid model, Nuclear Science and Engineering 89 (1985) 197–206.

[6] J.H. Stuhmiller, The influence of interfacial pressure forces on the characteristics of two-phase flow model equations, International Journal of Multiphase Flow 3 (1977) 551–560.
[7] H. Pokharna, M. Mori, V.H. Ransom, Regularization of two-phase flow models: a comparison of numerical and differential approaches, Journal of Computational Physics 134 (1997) 282–295.
[8] K.W. Morton, Numerical Solution of Convective-Diffusion Problems, Chapman & Hall, London, 1996.
[9] J.A. Trapp, R.A. Riemke, A nearly-implicit hydrodynamic numerical scheme for two-phase flow, Journal of Computational Physics 66 (1986) 62–82.
[10] S. Burge, RELAP5/MOD3.11, Dynamic Stability Simulations and Code Improvements, RELAP5 Users Meeting, Dallas, 1996.
[11] P.J. Roache, Fundamentals of Computational Fluid Dynamics, Hermosa Publisher, 1998.
[12] G.H. Golub, C.F. Von Loan, Matrix Computation, John Hopkins University Press, Baltimore, MD, 1983.
[13] R.F. Warming, B.J. Hyett, The modified equation approach to the stability and accuracy of finite difference methods, Journal of Computational Physics 14 (1974) 159–179.
[14] C. Hirsch, Numerical Computational of Internal and External Flows, Wiley, New York, 1990.
[15] B. Van Leer, Toward the ultimate conservative difference scheme V. A second order sequel to the Godonov's method, Journal of Computational Physics 32 (1979) 101–136.
[16] P.K. Sweby, High resolution schemes using flux limiters for hyperbolic conservation laws, SIAM Journal of Numerical Analysis 21 (1984) 995–1011.
[17] P.L. Roe, Approximate Riemann solvers, parameter vectors and difference schemes, Journal of Computational Physics 43 (1981) 357–372.
[18] S.M. Cox, P.C. Matthews, Exponential time differencing for stiff systems, Journal of Computational Physics 176 (2002) 430–455.
[19] A. Harten, J.M. Hyman, Self adjusting grid methods for one-dimensional hyperbolic conservation laws, Journal of Computational Physics 50 (1983) 235–269.